Reply to Reviewers' Comments

We thank the referees for their time and efforts. Their constructive comments and suggestions helped to improve the overall quality of the manuscript.

We now summarize the changes in the manuscript, as a result of the suggestions of the referees. The referee report is cited, followed by our answers.

Referee 1:

Importance:

Hypotheses Yes/No:

Appropriate Length:

Different Journal:

Recommend Acceptance: B) Yes, with minor alterations

Referee Letter: This manuscript reports the catalytic activity of a gallium metal organic framework in where the linker acts as ligand of Cu2+ ions for the oxidation of cyclohexene. The system uses molecular oxygen as terminal oxidant and over stoichiometric amounts of aldehyde as mediator. The authors have performed some (no such relevant) calculations of the optical spectrum of a simple Cu2+ complex as simple model to compare the optical spectrum of the Cu2+ in the MOF. The authors reach a high selectivity towards the wanted epoxide product. This work can be recommended for publication with some changes addressing the following comments:

1. *What is the fact of isoburaldehyde? Is the corresponding acid formed in stoichiometric amounts with respect to cyclohexene oxidation? Can the excess of this aldehyde be reduced? Is the carboxylic acid a poison of the catalyst?*

Author reply: In this reaction, isobutyraldehyde is a co-reactant, it is transformed in situ into an acylperoxy radical (eq 2), which is the predominant oxidizing species, facilitating the oxygen transfer to the cyclohexene. The corresponding carboxylic acid is not formed in stoichiometric amounts with respect to cyclohexene oxidation. As can be seen in Scheme 1 below, the acylperoxy radical can react with the aldehyde to form a peroxy acid and an acyl radical (eq 3). The peroxy acid is a competing epoxidizing agent generating the carboxylic acid in a nonradical epoxidation pathway (eq 4). On the other hand, the peroxy acid can react further with the aldehyde to form two molecules of carboxylic acid (eq 5).

Faculty of Sciences – Department of Inorganic and Physical Chemistry
Krijgslaan 281 S3, B-9000 Gent (Belgium)

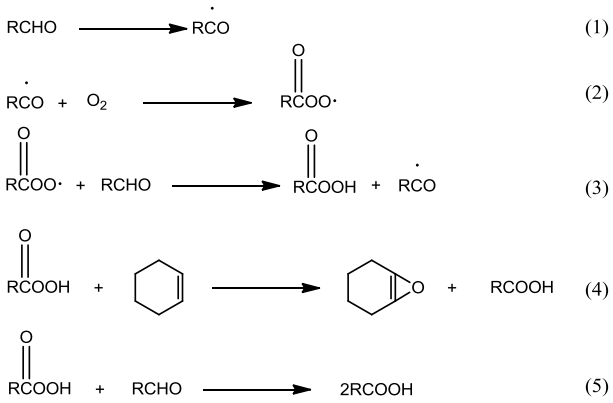

Scheme 1

The excess of the aldehyde helps to accelerate the reaction rate. When the amount is reduced the conversion will be less under the same conditions, however, the selectivity will not be influenced. We chose the ratio of aldehyde: reactant =2:1, which is the best ratio to maintain a high reaction speed while the blank test without the catalyst still shows zero epoxide formation. Carboxylic acid does not poison the catalyst, as the catalyst has been tested for 4 runs and the catalytic activity expressed as TOF remains constant during the 4 runs (Figure 7(bottom) in Page 4 maintext).

2. *Optical absorption spectra of the solids have been recorded in suspension after sonication. This is a strange method and could explain why the authors have been unable to record the d-d transitions of Cu2+ in the visible. The authors should re-record the UV-Vis absorption spectra using a conventional diffuse reflectance set-up and show the presence of this band in the visible region. Otherwise, the mismatch between the calculations predicted for the model, the observation of color in the material and the absence of visible absorption band is apparent. Moreover, how can the authors state on page 3, left that the two bands at 338 and 450 nm can be employed to reveal the successful incorporation of CuCl2 when is not seen in the spectrum of the solid?*

Author reply: We thank the referee for the suggestion. We have performed UV-Vis DRS measurement as shown in the figure below. The results are now included on pages 2 and 3 of the revised manuscript: “DRS measurements have also been performed on powder samples in order to get better resolution in the visible region. As shown in figure 2 (bottom), COMOC-4 gives a broad weak absorption band in the range of 430~500 nm, whereas after incorporation of Cu^{2+} cations, a well distinguishable absorption band centered at 460 nm is recorded.” The instrumental information is included in the experimental section of the manuscript: “The UV−Vis diffuse reflection spectra (DRS) experiments were carried out using Hitachi U-3000 UV-VIS Spectrophotometer with diffuse reflectance accessory (integrated sphere) for spectrophotometric measurements in the range of 350−800 nm. The spectra were converted using the Kubelka−Munk function.”

Faculty of Sciences – Department of Inorganic and Physical Chemistry
Krijgslaan 281 S3, B-9000 Gent (Belgium)

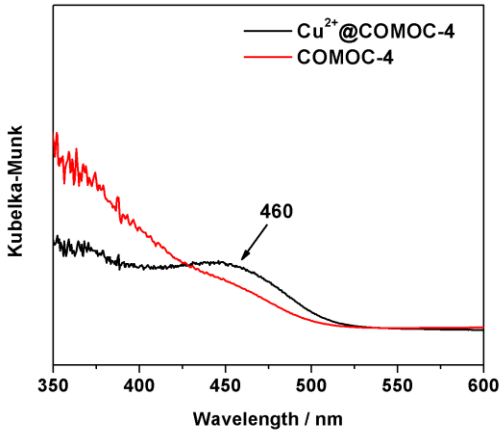

Figure 2(bottom). Solid-state UV−Vis spectra calculated from diffuse reflection spectra

3. *Concerning Fig. 6, the authors indicate some decomposition temperatures that do not agree well with the plot. In addition, they should comment on the lower stability of the material after incorporation of Cu2+.*

Author reply: We rewrote the paragraph on page 4 of the manuscript: “As can be seen from Figure 6, for the COMOC-4 material, the first mass loss in the TGA profiles corresponds to the elimination of water from the pores (~6.5 wt %). COMOC-4 is thermally stable up to 300 ^{0}C, above which a further weight loss of 62 wt % before 560 °C is indicative for the decomposition of the framework. The final residue (observed: 29.6 wt %, calculated 26.6 wt %) is Ga_2O_3. The incorporation of Cu^{2+} decreases the thermal stability of the MOF framework; a similar behavior was observed in Ru@MOF-253 [F. Carson et al., *Chem. Eur. J.*, 2012, **18**, 15337-15344.]. It should be noted that the TGA profile of Cu^{2+}@COMOC-4 is of the as-synthesized sample, the TGA curve shows a consistent weight loss of 11.5 wt% of solvent (water, methanol) release in the initial stage, the delayed release (up to 200 °C) can be assigned to the weakly bound methanol molecules, which are presumably held by weak forces (hydrogen bonds and van der Waals interactions) within the channels of the main framework as well as water molecules which are more firmly bound to the $CuCl_2$. A second major weight loss (62.5 wt%) occurs at 230 °C, which is attributed to the framework decomposition. The residue of 26.1 wt% (calculated: 27.6%) is Ga2O3 and CuO. Calculated values are based on the elemental analysis results.”

4. *Moreover, the XRD presented indicate a decrease in the crystallinity of COMOC-4 and some changes in the pattern after addition of Cu2+ ions. These observations need to be commented and the reason for this behavior should be proposed.*

Author reply: The main difference is seen in the diffraction peak at 6.5^{0}, this diffraction peak is related to the (101) planes which are parallel to the linkers (both directions are equivalent due

Faculty of Sciences – Department of Inorganic and Physical Chemistry
Krijgslaan 281 S3, B-9000 Gent (Belgium)

to symmetry). The incorporation of $CuCl_2$ will induce slight changes in the shape and angle of the linkers, and as a consequence the bragg planes will also be moved closer or further together. However not all the linkers are modified, meaning not all the planes are influenced the same. This results in several new bragg reflections close to the original ones which are then merged together in one broader peak of lower intensity as observed in the XRD pattern.
We rewrote the corresponding paragraph of page 2: "The Bragg diffraction angles in COMOC-4 and Cu^{2+}@COMOC-4 are essentially identical, confirming that the COMOC-4 crystalline structure is preserved. After Cu incorporation, the intensity of the reflections decreased. The main difference is seen in the diffraction peak at 6.5^0, this peak is related to the (101) planes which are parallel to the linkers (both directions are equivalent due to symmetry). The incorporation of $CuCl_2$ will induce slight changes in the shape and angle of the linkers. This results in several new bragg reflections close to the original ones which are then merged together in one broader peak of lower intensity as observed in the XRD pattern."

5. *The authors should indicate the occupation percentage of Cu2+ ions in the MOF. What is the influence of the Cu loading on the catalytic activity and selectivity? Has this been optimized?*

Author reply: The loading of Cu^{2+} ions used in this manuscript is: $(CuCl_2)_{0.4}$@COMOC-4, in which every 2.5 organic linker shares 1 Cu^{2+} ion.
In general, we have tested the loading of $CuCl_2$ in the range of 30%~40%. In this range the catalytic activity and selectivity is nearly the same. We didn't perform a systematic study on the influence of the Cu loading toward the catalytic activity and selectivity, this might be the topic of another investigation.

6. *Concerning the catalytic results, besides information at final time, the reader wants to see the time conversion plots. Of particular interest is the change in product selectivity along the conversion.*

Author reply: We agree with the referee and we have included the time to conversion plots of Cu^{2+}@COMOC-4 in the first run in the SI of the revised manuscript (Figure S4, see figure below)

Faculty of Sciences – Department of Inorganic and Physical Chemistry
Krijgslaan 281 S3, B-9000 Gent (Belgium)

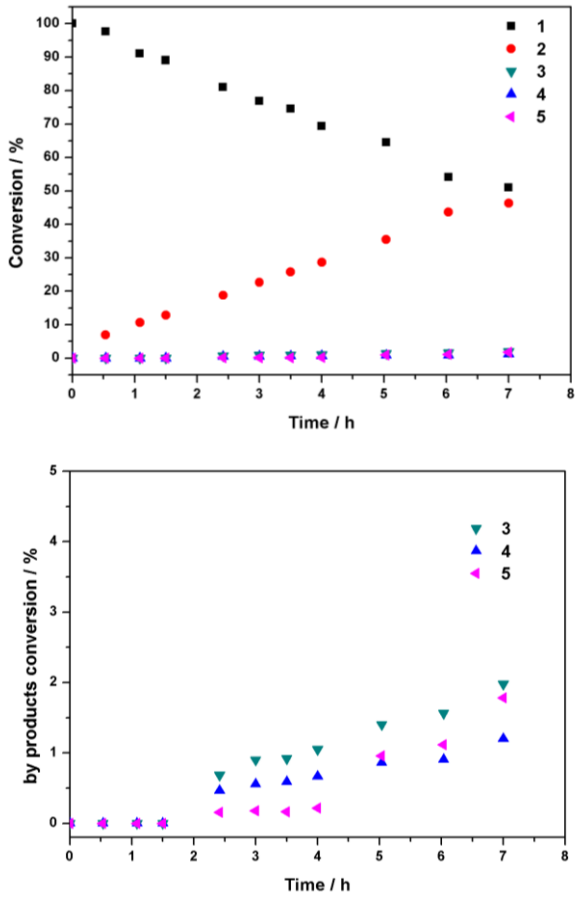

Figure S4. Left: Time conversion of cyclohexene (**1**) and time evolution of product distribution (cyclohexene oxide (**2**), 2-cyclohexene-1-one (**3**), 2-cyclohexen-1-ol (4) and cyclohexane-1,2-diol (**5**)) over Cu^{2+}@COMOC-4 during the 1st run. Right: detailed time evolution of by-product distribution over Cu^{2+}@COMOC-4 during the 1st run.

7. Table 1 should be completed adding catalytic data of the homogeneous Cu2+ complex.

Author reply: We tested the cataytic performance of the $Cu[Me_2bpydc]Cl_2$ complex under the same reaction conditions. However, this complex does not have a good solubility in the reaction mixture. Only 9.2% of the Cu complex was dissolved in chloroform. Therefore, the catalytic performance of the complex is due to the contribution of both heterogeneous and homogeneous catalysis. The Cu complex catalyzed cyclohexene conversion is 33.4% and the selectivity towards the epoxide is 88%. In comparison, the Cu@COMOC-4 catalyzed cyclohexene conversion is 49% in the 1^{st} run, while the selectivity is 89%. The lower conversion observed in the Cu complex is due to the fact that this solid $Cu[Me_2bpydc]Cl_2$ complex is a nonporous material with a condensed structure. Therefore the accessible Cu sites are limited in contrast to the highly porous Cu^{2+}@COMOC-4 material. In conclusion, due to the solubility issues, the catalytic result of the Cu complex can not provide a fair comparison with the result of Cu^{2+}@COMOC-4, therefore, we decide not to include this part of discussion in the manuscript.

Faculty of Sciences – Department of Inorganic and Physical Chemistry
Krijgslaan 281 S3, B-9000 Gent (Belgium)

8. Typically MOfs are activated before the reaction. Since the authors have not performed solid activation, they have to provide catalytic data showing that the initial reaction rate and final conversions are the same for a catalyst with and without adequate activation.

Author reply: All the fresh catalysts were activated under vacuum at 120 ^{o}C for 3 h prior to catalysis. After each catalytic run, the catalyst was recovered by filtration, washed with acetone and dried at room temperature overnight under vacuum to reuse it in a next run. The catalytic results showed that the catalyst maintained a good catalytic activity during these 4 runs, indicating no catalyst reactivation was needed before reuse. We have rewritten the experimental section to clarify this part (page 7 of the manuscript).

Referee 2:

Importance: C) important

Hypotheses Yes/No: Yes

Appropriate Length: Yes

Different Journal:

Recommend Acceptance: B) Yes, with minor alterations

Referee Letter: Given the difficulty in obtaining MOFs that are competitive catalysts, the main result found by the authors is that COMOC-4 does not leach in the reported reaction, in contrast to the previously reported case of another MOF, HKUST-1, which leaches as much as 13%.

A few points must be addressed before the manuscript is accepted for publication in ChemCatChem.

1. *The text (page 3) commenting on Figure 6 indicates that Cu-COMOC-4 starts to decompose after 250 ºC. However, an earlier step down appears between 100-200 ºC, suggesting some kind of defects formation in the material. Further comments on this aspect would contribute to clarify the stability of Cu-COMOC-4.*

Author reply: We rewrote the paragraph on page 4: “As can be seen from Figure 6, for the COMOC-4 material, the first mass loss in the TGA profiles corresponds to the elimination of water from the pores (~6.5 wt %). COMOC-4 is thermally stable up to 300 ^{o}C, above which a further weight loss of 62 wt % before 560 °C is indicative for the decomposition of the framework. The final residue (observed: 29.6 wt %, calculated 26.6 wt %) is Ga_2O_3. The

Faculty of Sciences – Department of Inorganic and Physical Chemistry
Krijgslaan 281 S3, B-9000 Gent (Belgium)

incorporation of Cu^{2+} decreases the thermal stability of the MOF framework; a similar behavior was observed in Ru@MOF-253 [F. Carson et al., *Chem. Eur. J.*, 2012, **18**, 15337-15344.]. It should be noted that the TGA profile of Cu^{2+}@COMOC-4 is of the as-synthesized sample, the TGA curve shows a consistent weight loss of 11.5 wt% of solvent (water, methanol) release in the initial stage, the delayed release (up to 200 °C) can be assigned to the weakly bound methanol molecules, which are presumably held by weak forces (hydrogen bonds and van der Waals interactions) within the channels of the main framework as well as water molecules which are more firmly bound to the $CuCl_2$. A second major weight loss (62.5 wt%) occurs at 230 °C, which is attributed to the framework decomposition. The residue of 26.1 wt% (calculated: 27.6%) is Ga2O3 and CuO. Calculated values are based on the elemental analysis results."

2. *Figure 1 seems to refer only to Cu-COMOC-4 and not to COMOC-4, hence the Ga should not be present in the atom list. Secondly, the Figure is too small to allow appreciation of details: a larger version could be included in the supplementary information.*

Author reply: We have made the suggested corrections to Figure 1 and added an extra figure with more details in the supporting information (Figure S2).

3. *The notation Cu@COMOC-4 seems to indicate clusters of metallic Cu(0) occluded in COMOC-4. I suggest Cu-COMOC-4 unless the authors do have a justification for their notation choice.*

Author reply: We have used Cu^{2+}@COMOC-4 in the entire manuscript to avoid confusion.

4. *Numerical data showing the % participation of Cu (and linker) in the molecular orbitals of Figure S4 would contribute to further clarify the important point made by the authors, that the peak calculated at 450 nm is a Metal-to-Ligand transition. In relation to this, Figure 4 needs improved resolution.*

Author reply: We thank the referee for this comment and the suggested information is added in the supporting information of the revised manuscript. The original Figure and text has been replaced by the Figure and discussion as given hereafter. Relevant orbitals indicating the metal-to-ligand transition are also included in Figure 4 of the revised manuscript.

'In order to determine if the changes in the calculated UV/Vis spectrum are a consequence of the metal coordination, the molecular orbitals corresponding to the extra bands in the absorption spectrum were visualized. Figure S3(a) displays the theoretical UV/Vis spectrum of a the cupper-modified linker. The spectrum was calculated for the optimized geometry using TD-DFT, in particular B3LYP/6-311+G(d).
Three peaks can be distinguished, with maxima around 403, 324 and 307 nm. These values deviate from the values of the averaged MD spectrum (see Figure 4 in the main manuscript)

Faculty of Sciences – Department of Inorganic and Physical Chemistry
Krijgslaan 281 S3, B-9000 Gent (Belgium)

since it corresponds with one particular geometry, however the overall shape of the spectrum is maintained. This behavior is explained in more detail in refs. [T. De Meyer, K. Hemelsoet, L. Van der Schueren, E. Pauwels, K. De Clerck, V. Van Speybroeck, Chem. – A Eur. J. 2012, 18, 8120; K. Hemelsoet, Q. Qian, T. De Meyer, K. De Wispelaere, B. De Sterck, B. M. Weckhuysen, M. Waroquier, V. Van Speybroeck, Chem. – A Eur. J. 2013, doi: 10.1002/chem.201301965].

We focus on the absorption at 403 and 324 nm, which are due to the metal coordination. Investigation of the underlying transitions reveals that a variety of orbitals is involved. However, the feature at 403 nm mainly results from a HOMO to LUMO transition (in particular orbitals 103a and 104a are involved, see Figure S3(b)). The peak at 324 nm is mainly due to a transition from orbital 100a to 104a as well as from 100b to 104b (Figure S3(c)). The involved orbitals are depicted and the participation of the $CuCl_2$ and linker fragments in the oribitals are also given. From this information, it is clear that the observed peaks involve a metal-to-ligand transition.'

Faculty of Sciences – Department of Inorganic and Physical Chemistry
Krijgslaan 281 S3, B-9000 Gent (Belgium)

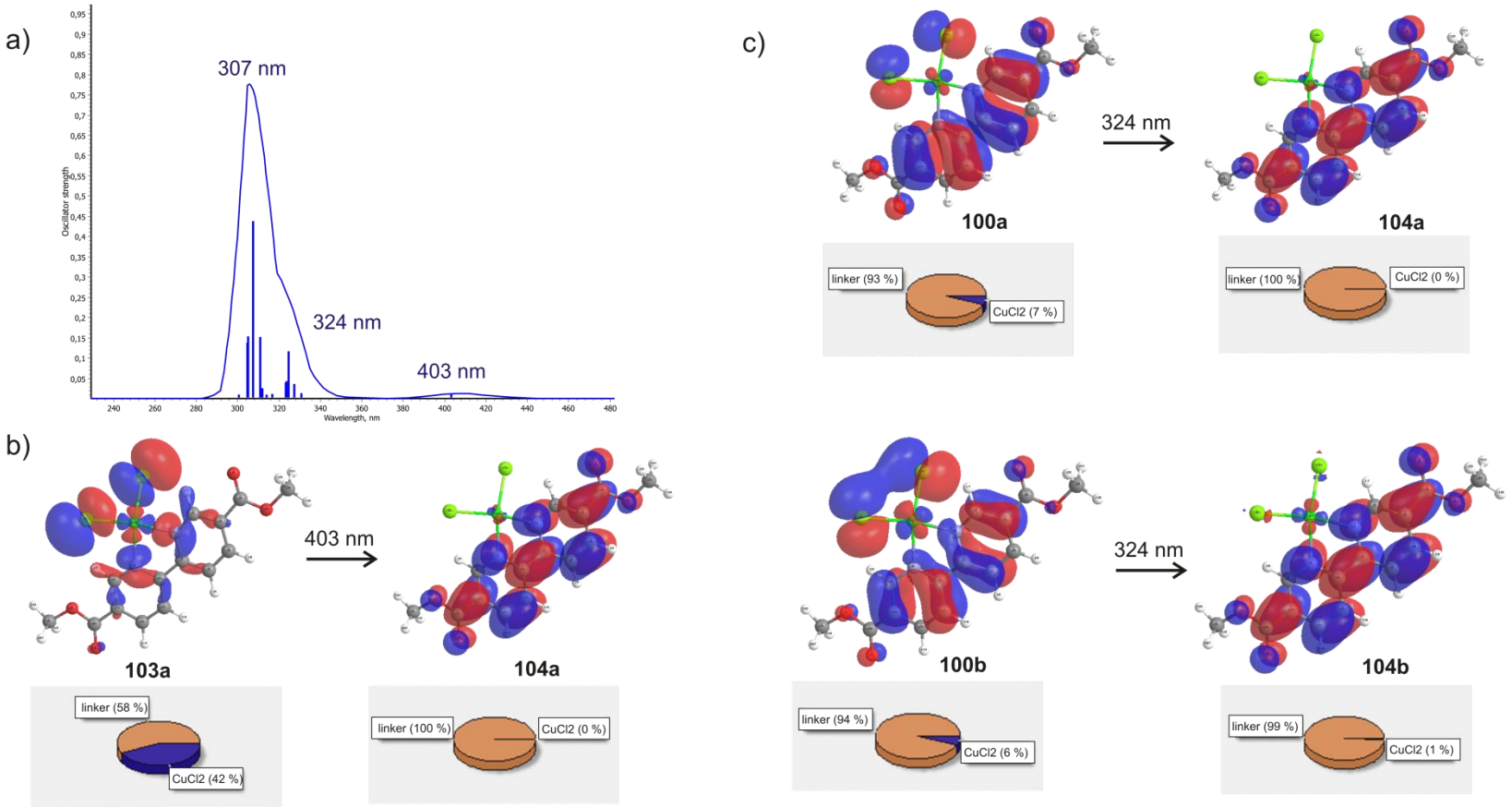

Figure S3 (a) Theoretical UV/Vis spectrum of the Cu-modified linker, calculated for a snapshot extracted from the MD simulation. (b) Iso-surfaces of dominant orbitals involved in the excitation at 403 nm. (c) Iso-surfaces of the dominant orbitals involved in the excitation at 324 nm.The participation of the separate fragments are also depicted; in particular in orange for the linker and in blue for the $CuCl_2$.

Faculty of Sciences – Department of Inorganic and Physical Chemistry
Krijgslaan 281 S3, B-9000 Gent (Belgium)

Referee 3:

Importance: D) less important

Hypotheses Yes/No: No

Appropriate Length:

Different Journal: Eur. J. inorg. Chem. (after major revision)

*Recommend Acceptance: D) No *)*

Referee Letter: Van der Voort et al. present a bimetallic-organic framework as catalyst in aerobic epoxidation of cyclohexene. Due to the following issues I cannot recommend the manuscript for publication in the present form. The contribution might be suitable for another journal like Eur. J. Inorg. Chem. after the following points have been addressed by the authors:

1) *The PXRD pattern shown in Figure S1 have very broad reflexes and a high noise level, probably due to low crystallinity and the obtained surface area is much lower (only 920 m2/g) than would be expected for materials with accessible pores. Do the authors have an explanation for these two observations? How can they exclude that additional unwanted phases may be present, which might be responsible for catalytic activity?*

Author reply: As shown in the figure A below, TEM and SEM images have demonstrated that COMOC-4 crystalline compounds are in the nanosize range, consisting of irregularly-shaped, crystalline nanoplates with fairly uniform sizes of approximately 30~50 nm. These crystalline nanoparticle sizes are consistent with the line broadening of the XRD peaks, as explained by the Sherrer equation. Futhermore, the TGA together with EA results clearly confirmed the purity of the COMOC-4. The chemical formula is $Ga(OH)(C_{12}H_6N_2O_4)\bullet 2.7H_2O$ with no indication of unreacted linker or DMF left in the COMOC-4 framework. XRD pattern also shows no additional peaks representing other phases. The main difference is seen in the diffraction peak at 6.5^0, this diffraction peak is related to the (101) planes which are parallel to the linkers (both directions are equivalent due to symmetry). The incorporation of CuCl2 will induce slight changes in the shape and angle of the linkers, and as a consequence the bragg planes will also be moved closer or further together. However not all the linkers are modified, meaning not all the planes are influenced the same. This results in several new bragg reflections close to the original ones which are then merged together in one broader peak of lower intensity as observed in the XRD pattern.

We rewrote the corresponding paragraph of page 2: “The Bragg diffraction angles in COMOC-4 and Cu2+@COMOC-4 are essentially identical, confirming that the COMOC-4 crystalline structure is preserved. After Cu incorporation, the intensity of the reflections decreased. The main difference is seen in the diffraction peak at 6.5^0, this peak is related to the (101) planes which are parallel to the linkers (both directions are equivalent due to symmetry). The incorporation of CuCl2 will induce slight changes in the shape and angle of the linkers. This results in several new bragg reflections close to the original ones which are then merged together in one broader peak of lower intensity as observed in the XRD pattern.”

We also tested the catalytic activity of COMOC-4 , as shown in the Table 1 of the manuscript, the conversion of cyclohexene is 11.4%, with 52.5% selectivity toward the epoxide. This can be attributted to the Ga lewis acid sites of the MOF framework.

Faculty of Sciences – Department of Inorganic and Physical Chemistry
Krijgslaan 281 S3, B-9000 Gent (Belgium)
www.we06.ugent.be/comoc

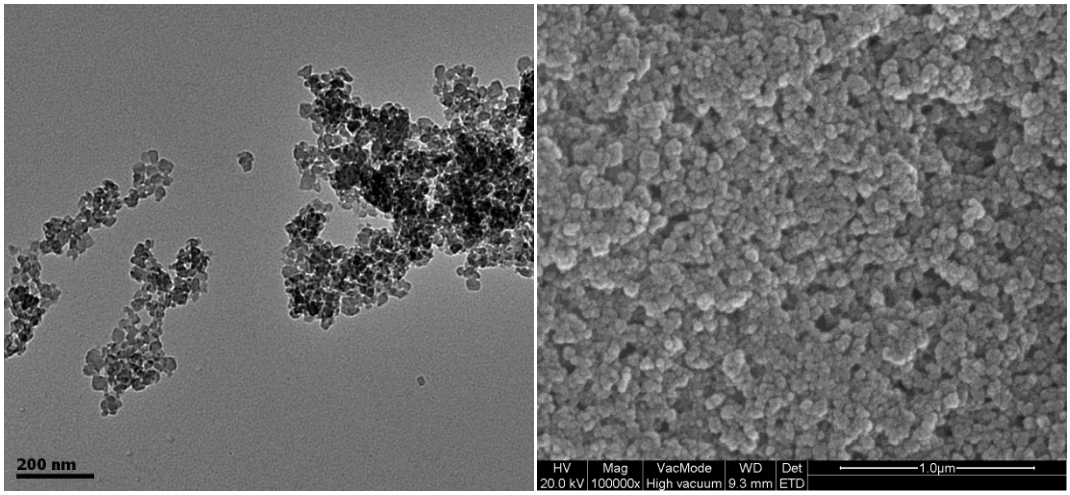

Figure A. TEM(left) and SEM(right) micrographs of COMOC-4 nanocrystals

2) *There is no experimental evidence for the incorporation of Cu in the desired way. Do the authors have any information on the nature of the Cu species (chelated Cu ions vs. nanoparticle formation) in the material based on experimental data?*

Author reply: This is a good suggestion of the referee and we have checked the molar ratio of chlorine and copper, Cl/Cu=2.2. As there is no extra chlorine source introduced during the synthesis, no chlorinated reagents or solvents have been used, and the materials are thoroughly washed after modification, all Cl-ligands are from the tethered $CuCl_2$. The result confirmed the Cu species are present as chelated Cu^{2+}.

3) *Both model structures were optimized using B3LYP/6-311+g(d), which does not account for relativistic effects. Therefore this computational method is not suitable for the Cu containing structure.*

Author reply: We thank the referee for this comment. First of all, it is important to point out that a set of deformed geometries is generated using a MD simulation involving the BLYP functional. The subsequent TDDFT simulations are indeed done using the B3LYP/6-311+G(d) level of theory. We believe this method is adequate to model the systems under investigation, since we are aiming at describing the difference between the parent and modified linker. In this light, we refer to a study of Ghost et al. [A. Alemayehu, J. Conradie and A. Ghosh, *Eur. J. Inorg. Chem.*, 2011, 2011, 1857-1864.] who report on the successful use of B3LYP with a standard basis set on copper complexes for TDDFT calculations.

However, we agree with the referee that relativistic contributions are necessary when results of high quantitative accuracy are targeted. A thorough investigation on this topic is outside the scope of this paper, however a brief this discussion is added in the supporting information of the revised version of the manuscript. To assess the influence of relativistic contributions on our results, additional simulations were performed using the Orca program. Relativistic effects were explicitly taken into account using the ZORA option. This methodology is similar to the one used by Ji et al. [M. Ji, Z. Lan, Z. Han, C. Hao and J. Qiu, Inorg. Chem. 2012, 51, 12389] for the simulation of luminescent properties of MOF-5.

Table S1 lists the important absorption peaks of the Cu-modified linker. In addition to testing the influence of relativistic effects, also the performance of two basis sets (in particular SVP and TZVPP) and the BLYP and B3LYP functionals were assessed. This is necessary, since a straightforward comparison with the original results is not straightforward due to the use of different software packages and implementations. We note that in the computed spectra a large number of excitations, with small oscillator strengths, is observed. The results in Table S1 correspond to the excitations with maximal oscillator strength in the region of interest (between

400-480 nm). We indeed observe a substantial shift between the values computed using the Gaussian (403nm; Figure S3) and Orca (close to 450 nm; Table S1) programs. The values of Table S1 are in closer agreement with the averaged MD result (see Figure 4 of the main manuscript); a full analysis is however outside the scope of this paper.

Table S1. Computed excitation energies [in nm] for the Cu-modified bipyridine linker.

	Cu-bipyridine			
	BLYP		B3LYP[a]	
	Without ZORA	With ZORA	Without ZORA	With ZORA
SVP	454	457	460	453
TZVPP[a]	453	452	-	-

[a] The B3LYP/TZVPP simulations are computationally too demanding for the Cu-modified linker

Importantly, the additional simulations support the observation that relativistic effects do not substantially change the qualitative behavior of the optical spectrum of the Cu-modified linker, a maximal shift of 7 nm is obtained between the results with and without ZORA effects. This conclusions suggests that the original methodology (i.e. TDDFT simulations using the B3lYP/6-311+G(d) level of theory) succeeds at describing the systems under investigation.

4) The authors should include relevant references on oxidation reactions catalyzed by other MOF catalysts (some recent examples: J. Catal. 2013, 298, 61; Chem. Eur. J. 2013, 19, 1986; ACS Catal. 2013, 3, 647; Appl. Catal. A, 2013, 455, 261; Catal. Sci. Technol. 2013, 3, 371; J. Catal. 2012, 289, 259; Chem. Eur. J. 2012, 18, 887; Chem. Commun. 2012, 48, 6812). The results presented in the present manuscript should be critically discussed and compared to these literature examples.

Author reply: We agree with the referee on this comment. We have included the references in Page 4 of the manuscript: "The aerobic epoxidation of cyclohexene within the presence of an aldehyde as co-oxidant was used in this study. Such liquid phase oxidation of cycloalkenes (or cycloalkanes) has been intensively studied using MOF based material as catalyst. With variable active sites on MOF catalysts, and the use of different oxidants, this reaction can lead to different product distributions.[16a, 16b, 16c, 16d, 16e, 16f]. Kholdeeva and co-workers[16f] reported a Cr- and Fe-MIL-101 as catalyst for solvent-free selective oxidation of cyclohexane with O_2 and/or tert-butyl hydroperoxide(TBHP) as oxidant. The substrate conversion was in the range of 9~36 % within 8h, the major product formed can be cyclohexyl hydroperoxide or cyclohexanone. This strongly depends on the nature of the active metal. Kleist and co-workers[16a] investigated the aerobic epoxidation of olefins ((*E*)-stilene and styrene) in a basic solvent (dimethylformamide, DMF), catalyzed by a Co based MOF (STA-12(Co)). Different selectivities were obtained depending on the substrates. The selectivity in styrene epoxidation was low due to the substrate oligomerization. However, (*E*)-stilene was epoxidized with hight selectivites between 80%~90%. Garcia and co-workers[16b] reports the aerobic oxidation of cyloalkenes catalyzed by Fe based MOF, in the presence of N-hydroxyphthalimide, the cycloalkenes give major conversion of allylic oxdiation products. More recently, Xamena, Corma and co-workers[16e] reports the MOFs with Cu^{2+} centers linked to four nitrogen atoms from azaheterocyclic compounds, are active catalysts for aerobic oxidation of activated alkanes. Furthermore, a tandem reaction was designed using Cu-MOF combined with silylated Ti-MCM-41 as solid catalyst, in which Cu-MOF first catalyzed cumene oxidation to form cumene hydroperoxide as major product, the intermediate hydroperoxide, together with silylated Ti-MCM-41 further catalyzed 1-octene to obtain 1-octene oxide. However, at high temperature (90 ^{o}C) the presence of Cu-MOF will catalyze the 1-octene to allylic reaction, therefore, to increase the selectivity to the epoxide product, 1-octene and the Cu-MOF was kept at separate reactors. In the present work, we further explore the catalytic activity of the Cu-MOF in the epoxidation of alkene by the 'Mukaiyama' system.[17]
The related discussions are included and highlighted in red in Page 4, 5 of the main text.

DOI: 10.1002/cctc.200((will be filled in by the editorial staff))

Cu^{2+}@COMOC-4: a bimetallic-organic framework as zero-leaching catalyst in the aerobic oxidation of cyclohexene

Ying-Ya Liu,[a] Karen Leus,[a] Thomas Bogaerts,[a,b] Karen Hemelsoet,[b] Els Bruneel, [c] Veronique Van Speybroeck[b] and Pascal Van Der Voort*[a]

A gallium 2,2′-bipyridine-5,5′-dicarboxylate metal-organic framework, denoted as COMOC-4, has been synthesized via a solvothermal synthesis procedure. This MOF compound exhibits the same topology as MOF-253. By means of a post-synthetic modification (PSM), $CuCl_2$ was incorporated into COMOC-4. The spectroscopic absorption properties of the MOF framework before and after PSM were compared with theoretical data employing molecular dynamics combined with time-dependent density functional theory (TD-DFT) calculations on both the as-synthesized and functionalized linker. The catalytic behavior of the resulting Cu^{2+}@COMOC-4 material was evaluated in the aerobic oxidation of cyclohexene applying isobutyraldehyde as a co-oxidant. In addition, the catalytic performance of the Cu^{2+}@COMOC-4 was compared with the commercially available Cu-BTC MOF. The Cu^{2+}@COMOC-4 material exhibits a good cyclohexene conversion and an excellent selectivity towards cyclohexene oxide in comparison to the Cu-based reference catalyst. Furthermore, no leaching of the active Cu sites was noticed during at least 4 consecutive runs.

Introduction

Catalyzed liquid phase oxidation reactions are widely employed in industrial processes and are becoming more and more important for the synthesis of fine chemicals.[1a, 1b] Among the different oxidation reactions, the epoxidation of olefins plays a prominent role, as epoxides are highly reactive and versatile intermediates. Although homogeneous catalysts are still often utilized in industrial processes, there is an increasing interest in the employment of heterogeneous catalysts as they have a big advantage in terms of reuse and minimizing the waste. Metal-organic frameworks (MOFs) can be considered as potential candidates for use in catalysis.[2a, 2b, 2c] MOFs are three dimensional crystalline porous materials, consisting of metal nodes that are connected by multifunctional organic linkers. Almost every transition metal ion and many different organic linkers can be used to obtain a MOF structure, what makes the plausible metal-ligand combinations endless [3a, 3b]. However, only a minor amount of MOFs are practically usable in catalysis, as many of them show a limited stability in the typically employed catalytic reaction conditions [4a, 4b, 4c]. By a pre-/post-synthetic modification of the organic linker, complementary catalytic active sites can be introduced [5a, 5b, 5c]. Very recently we reported on the post-modification of V-NH_2-MIL-47 with $TiO(acac)_2$. The resulting NH_2-MIL-47[Ti] exhibited a significantly higher stability and activity in the oxidation of cyclohexene compared to the non-functionalized NH_2-MIL-47[6].

In this study we looked for another MOF support which is more rigid in comparison to NH_2-MIL-47. Within this context, the bipyridine based MOF-253, synthesized by Yaghi and co-workers.[7], is an excellent candidate to serve as a MOF support. The beauty of this Al(OH)(bpydc) ($bpydc^{2-}$ = 2,2′-bipyridine-5,5′-dicarboxylate) framework lies in the fact that the organic linkers are offering free 2,2′-bipyridine sites, which are often employed as chelating ligands in coordination chemistry. More specifically, it can form metal-complexes in which the metal is bounded to the two nitrogen atoms, making it a bidentate secured stable complex. Several attempts have been made to graft secondary metal sites on the bipyridine site by a post-synthetic modification approach. For example, Pd^{2+} and Cu^{2+} ions have been incorporated into the MOF-253 framework and were subsequently evaluated for their CO_2 uptake[7]. Zou and co-workers have incorporated $RuCl_3$ on MOF-253, which was examined as a catalyst for the selective oxidation of primary and secondary alcohols.[8] In a very recent report of Li et al, Cu^+ ions were incorporated into MOF-253 to catalyze the cross-coupling of phenols and alcohols with aryl halides [9].

In this contribution, we report on the catalytic performance of

[a] *Dr. Y.-Y. Liu, Dr. K. Leus, T. Bogaerts, Prof. Dr. P. Van Der Voort*
COMOC - Center for Ordered Materials, Organometallics and Catalysis,
Department of Inorganic and Physical Chemistry,
Ghent University,
Krijgslaan 281-S3, 9000 Ghent; Belgium
Fax: (+)32-9-264.49.83, Tel: (+)32-9-264.44.42
E-mail: pascal.vandervoort@ugent.be
[b] *T. Bogaerts, Prof. Dr. K. Hemelsoet, Prof. Dr. V. Van Speybroeck*
Center for Molecular Modeling,
Ghent University,
Technologiepark 903, 9052 Zwijnaarde, Belgium
[c] *Dr. E. Bruneel*
SCRiPTs, Department of Inorganic and Physical Chemistry
Ghent University,
Krijgslaan 281-S3, 9000 Ghent, Belgium

Supporting information for this article is available on the WWW under http://dx.doi.org/10.1002/cctc.200xxxxxx.

a member of the M(OH)(bpydc)series with M = Ga, denoted as COMOC-4 (COMOC = Center for Ordered Materials, Organometallics and Catalysis, Ghent University) which we published very recently[10]. The MOF structure features an analogous structure to MOF-253 and is stable in air and water (50°C for 24h). The $CuCl_2$ complex, which shows a good binding affinity towards the bipyridine sites, was grafted on the COMOC-4 framework by means of a post-synthetic modification. The spectroscopic properties of the MOF before and after PSM were elucidated using ab initio simulations. In particular, molecular dynamics (MD) computations were performed on a model linker with and without Cu-coordination to simulate the flexibility of the structures. Subsequently, time-dependent density functional theory (TD-DFT) was applied on snapshots extracted from the MD runs to compute an average UV/Vis spectrum. This methodology was previously shown to be successful [11a, 11b]. The newly synthesized Cu^{2+}@COMOC-4 was extensively evaluated as a bimetallic catalyst in the aerobic epoxidation of cyclohexene within the presence of an aldehyde as co-oxidant[12a, 12b, 12c]. Additionally, regenerability and stability tests were carried out. Finally, the catalytic performance of Cu^{2+}@COMOC-4 was compared with another reference Cu- based MOF namely Cu-BTC.

Results and Discussion

The XRPD pattern of COMOC-4 (see Figure S1, supporting information) reveals that this framework is isostructural to the DUT-5 [13] (Al(OH)(bpdc)) ($bpdc^{2-}$ = biphenyl-4,4'-dicarboxylate) as well as to MOF-253 [7]. The structure is indexed with orthorhombic unit cell parameters of *a* = 21.98(24) Å, *b* = 7.302(8) Å, and *c* = 17.470(24) Å. As shown in Figure 1, the COMOC-4 framework is constructed of infinite chains of octahedral $GaO_4(OH)_2$ units, in which each Ga^{3+} ion is bound to four $bpydc^{2-}$ ligands and two μ_2 trans hydroxide anions. This is a common coordination motif that has already been observed in a series of M^{3+} carboxylate frameworks (M=Al, Fe, V, Ga and In). [14a, 14b] The $GaO_4(OH)_2$ chains are aligned parallel to the crystallographic *b* axis, with the hydroxide and the carboxylate moiety alternating on either side of the chains, further linked to each other to form a three dimensional open framework (Figure S2, supporting information). After the incorporation of $CuCl_2$ into the COMOC-4 framework, The Bragg diffraction angles in COMOC-4 and Cu^{2+}@COMOC-4 are essentially identical, confirming that the COMOC-4 crystalline structure is preserved. After Cu incorporation, the intensity of the reflections decreased. The main difference is seen in the diffraction peak at 6.5^0, this peak is related to the (101) planes which are parallel to the linkers (both directions are equivalent due to symmetry). The incorporation of $CuCl_2$ will induce slight changes in the shape and angle of the linkers. This results in several new bragg reflections close to the original ones which are then merged together in one broader peak of lower intensity as observed in the XRD pattern.

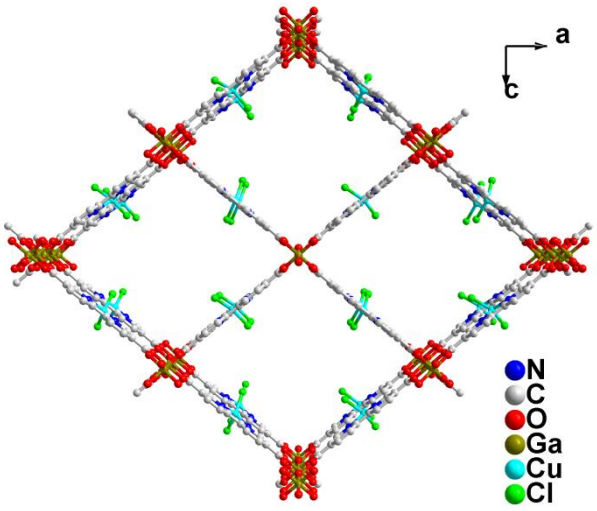

Figure 1. Representative structure of Cu^{2+}@COMOC-4. View along the one dimensional pore system. The structure model was generated based on the crystal structure of DUT-5 with 100% $CuCl_2$ occupancy. [13].

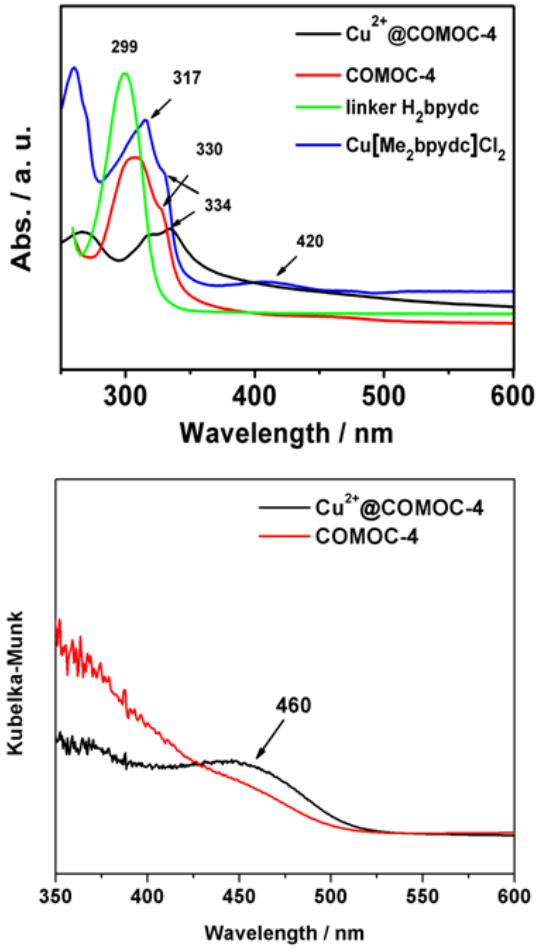

Figure 2. UV/Vis absorption spectra of suspended Cu^{2+}@COMOC-4 and COMOC-4 in MeOH solution compared to the $Cu[Me_2bpydc]Cl_2$ and Me_2bpydc ligand dissolved in MeOH solution(top); Solid-state UV−vis spectra calculated from diffuse reflection spectra (bottom).

The UV/Vis absorption spectra of the synthesized materials are presented in Figure 2 (top). As can be seen from this figure,

the H_2bpydc ligand displays one absorption band centered at 299 nm, arising from a π-π* transition in the aromatic rings. When the carboxylate linker is coordinated to gallium ions to form the COMOC-4 framework, the absorption spectrum exhibits a red-shift of ~8 nm. In addition, the absorption band reveals a shoulder at 330 nm. For comparison, the Cu[Me_2bpydc]Cl_2 is synthesized. As observed from the absorption spectra, the band corresponding to the organic ligand is red shifted to 317 nm, while a shoulder peak appears at 334 nm, a broad band at 420 nm is observed indicating the metal-to-ligand coordination. The Cu^{2+}@COMOC-4 material exhibits two band at respectively 317 and 334 nm, which are in agreement to the observed absorption bands of Cu[Me_2bpydc]Cl_2. However, the absorption band corresponding to the blue color is not visible due to the rather high background signal of the spectra recorded from the suspension. DRS measurements have also been performed on powder samples in order to get better resolution in the visible region. As shown in the Figure 2 (bottom), COMOC-4 gives a broad weak absorption bands in the range of 430~500 nm, whereas after incorporation of Cu^{2+} cations, a well distinguishable absorption band centered at 460 nm was recorded.

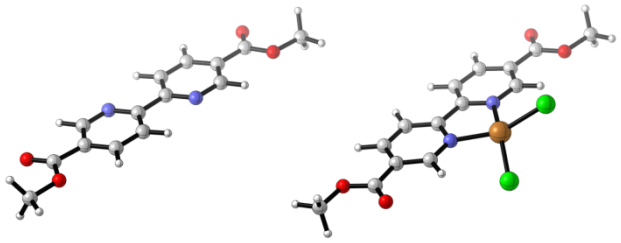

Figure 3. Optimized structure of the protected linker Me_2bpydc and the coordinated $CuCl_2$.

The model used for the empty linker is shown in Figure 3. This is the most stable conformation as we reported before.[10] To allow $CuCl_2$ to coordinate to this ligand both nitrogen atoms should be twisted to the same side as shown in Figure3. Both models were optimized using the B3LYP/6-311+g(d) methodology to find their most stable conformations. UV/Vis spectra were calculated using the computational method described below accounting for the flexibility of the structure. The main features from the experimental spectra are represented in the calculated dynamic spectra of Cu^{2+} coordinated to the bipyridine moiety compared with the as-synthesized linker. Figure 4a shows that there is a slight shift to higher wavelengths, from 309 to 315 nm, but the shift is smaller in comparison to the experimental spectrum (299-317 nm). The main absorption band for the empty linker (309 nm) is consistent with what was shown before with static calculations.[10] The shoulder at 338 nm (experimental: 334 nm) is also present and is a consequence of the Cu^{2+} encapsulation. The broad peak around 450 nm is also visible in the ab initio spectrum, though this is shifted to a higher wavelength as compared to the measured result. To confirm these changes are actually due to the metal coordination one can take a closer look at the molecular orbitals involved in these excitations. The dominant orbitals involved in the excitation around 450 nm are displayed in Figure 4b; full details can be found in the supporting information (Figure S3). The orbitals and corresponding participation of the different fragments (also shown in Figure 4b) indicate that the coordinated metal contributes to the electronic transition. We can thus conclude that the observed changes in the UV/Vis spectrum are due to the coordination of the $CuCl_2$ complex. The two bands at 338 nm and 450 nm can be employed to reveal the successful incorporation of $CuCl_2$ in the MOF framework, which was clearly observed on Cu^{2+}@COMOC-4 UV/Vis absorption spectra (334 nm) and UV/Vis DRS spectra (460 nm) (Figure 2 (bottom)).

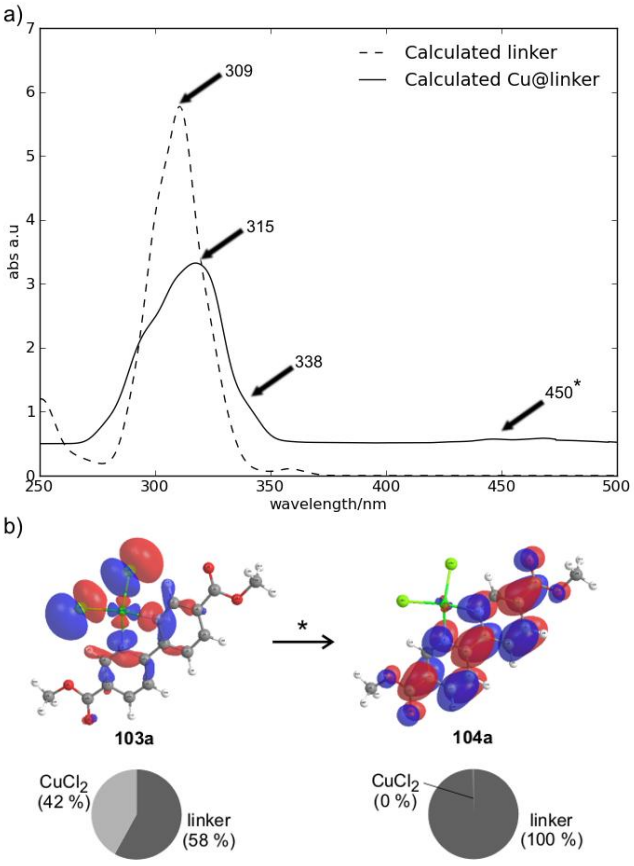

Figure 4. a) Comparison between the calculated UV/Vis spectra of the protected Me_2bpydc linker and copper coordinated to that linker. The most important features of the experimental spectrum are also indicated. b) Visualization of orbitals involved in the metal to ligand electron transfer corresponding to the visible excitation in the Cu-modified linker. The corresponding participation of the linker (in dark grey) and $CuCl_2$ (in light grey) fragments are also given.

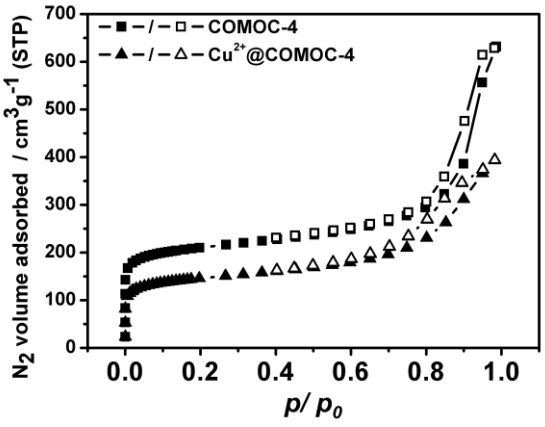

Figure 5. N_2 adsorption (solid symbols) and desorption (open symbols) isotherms of COMOC-4 and Cu2+@COMOC-4 at 77 K.

The COMOC-4 compound maintains a permanent micro porosity after removal of the guest molecules, as demonstrated by a type I N_2 sorption isotherm (Figure 5), exhibiting a Langmuir surface area of 920 m^2 g^{-1}. After the incorporation of $CuCl_2$, with a Cu/Ga ratio of 0.4/1, the $0.4Cu^{2+}$@COMOC-4 reveals a reduced Langmuir surface area of 630 m^2 g^{-1}. The thermal stability of COMOC-4 as well as $0.4Cu^{2+}$@COMOC-4 has been examined by means of TGA analysis (see Figure 6). As can be seen from this figure, for the COMOC-4 material, the first mass loss in the TGA profiles corresponds to the elimination of water from the pores (~6.5 wt %). COMOC-4 is thermally stable up to 300 °C, above which, a further weight loss of 62 wt % before 560 °C is indicative for the decomposition of the framework. The final residue (observed: 29.6 wt %, calculated 26.6 wt %) is Ga_2O_3. The incorporation of Cu^{2+} decreases the thermal stability of the MOF framework; a similar behavior was observed in Ru@MOF-253.[15] It should be noted that the TGA profile of Cu^{2+}@COMOC-4 is of the as-synthesized sample, the TGA curve shows a consistent weight loss of 11.5 wt% of solvent (water, methanol) release in the initial stage, the delayed release (up to 200 °C) can be assigned to the weakly bound methanol molecules, which are presumably held by weak forces (hydrogen bonds and van der Waals interactions) within the channels of the main framework as well as water molecules which are more firmly bound to the $CuCl_2$. A second major weight loss (62.5 wt%) occurs at 230 °C, which is attributed to the framework decomposition. The residue of 26.1 wt% (calculated: 27.6%) is Ga_2O_3 and CuO. Calculated values are based on the elemental analysis results.

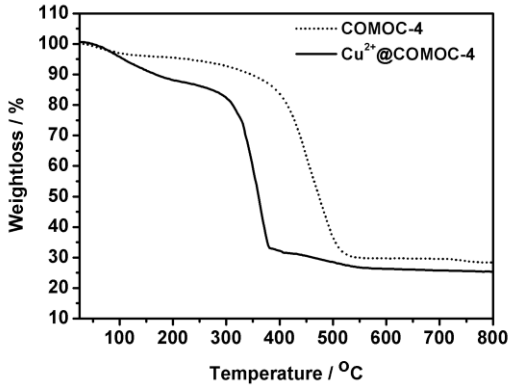

Figure 6. TGA curves of COMOC-4 and Cu^{2+}@COMOC-4 measured in an air flow.

The aerobic epoxidation of cyclohexene within the presence of an aldehyde as co-oxidant was used in this study. Such liquid phase oxidation of cycloalkenes (or cycloalkanes) has been intensively studied using MOF based material as catalyst. With variable active sites on MOF catalysts, and the use of different oxidants, this reaction can lead to different product distributions.[16a, 16b, 16c, 16d, 16e, 16f]. Kholdeeva and co-workers[16f] reported a Cr- and Fe-MIL-101 as catalyst for solvent-free selective oxidation of cyclohexane with O_2 and/or tert-butyl hydroperoxide(TBHP) as oxidant. The substrate conversion was in the range of 9~36 % within 8h, the major product formed can be cyclohexyl hydroperoxide or cyclohexanone. This strongly depends on the nature of the active metal. Kleist and co-workers[16a] investigated the aerobic epoxidation of olefins ((*E*)-stilene and styrene) in a basic solvent (dimethylformamide, DMF), catalyzed by a Co based MOF (STA-12(Co)). Different selectivities were obtained depending on the substrates. The selectivity in styrene epoxidation was low due to the substrate oligomerization. However, (*E*)-stilene was epoxidized with hight selectivites between 80%~90%. Garcia and co-workers[16b] reports the aerobic oxidation of cyloalkenes catalyzed by Fe based MOF, in the presence of N-hydroxyphthalimide, the cycloalkenes give major conversion of allylic oxdiation products. More recently, Xamena, Corma and co-workers[16e] reports the MOFs with Cu^{2+} centers linked to four nitrogen atoms from azaheterocyclic compounds, are active catalysts for aerobic oxidation of activated alkanes. Furthermore, a tandem reaction was designed using Cu-MOF combined with silylated Ti-MCM-41 as solid catalyst, in which Cu-MOF first catalyzed cumene oxidation to form cumene hydroperoxide as major product, the intermediate hydroperoxide, together with silylated Ti-MCM-41 further catalyzed 1-octene to obtain 1-octene oxide. However, at high temperature (90 °C) the presence of Cu-MOF will catalyze the 1-octene at allylic position. Therefore, to increase the selectivity to the epoxide product, 1-octene and the Cu-MOF was kept at separate reactors. In the present work, we further explore the catalytic activity of the Cu-MOFs in the epoxidation of alkene by the 'Mukaiyama' system.[17]

All our catalytic tests on the Cu-based MOFs were performed under identical reaction conditions to allow a fair comparison (see Table 1). Cu-BTC, a copper trimesate $Cu_3(BTC)_2(H_2O)_3$, known as HKUST-1, and commercially available as Basolite™ C300, was applied as a reference catalyst. This material forms face centered-cubic crystals that contain an intersecting three dimensional system of large square-shaped pores (9 × 9 Å).

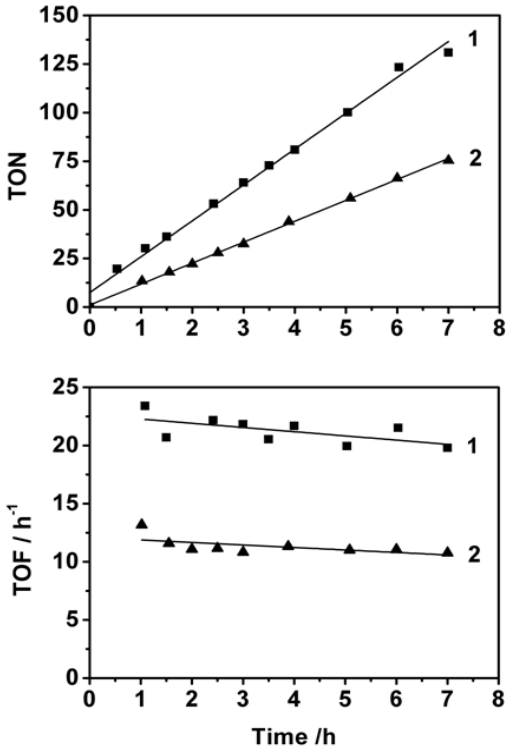

Figure 7. The catalytic activity expressed as TON (top) and TOF (bottom) for Cu^{2+}@COMOC-4 (1) and Cu-BTC (2). Reaction conditions: 0.2mmol Cu sites, 50 mmol cyclohexene, 100 mmol isobutyraldehyde, 40 mL chloroform, T =40 ◦C, O_2 flow: 7.7 ml/min

In Figure 7, the TON and TOF value of the two Cu-based MOFs is depicted as a function of the reaction time. As can be seen from this figure, Cu^{2+}@COMOC-4 and Cu-BTC, shows a good catalytic performance as evidenced by the linear increase in the TON number. Nevertheless, Cu^{2+}@COMOC-4 reveals a much higher TON value in comparison to Cu-BTC. After 7 hours of catalysis the TON value of Cu-BTC is 75 whereas Cu^{2+}@COMOC-4 exhibits a TON value of almost 138. Moreover, from Figure 7 (bottom) it can be seen that both catalysts reach a plateau in their TOF value after nearly one hour of catalysis. The TOF value of Cu-BTC is approximately 12 h^{-1} whereas for Cu^{2+}@COMOC-4 a significant higher TOF value of nearly 22 h^{-1} is noted which demonstrates that the latter catalyst converts the cyclohexene much faster in comparison to the reference catalyst.

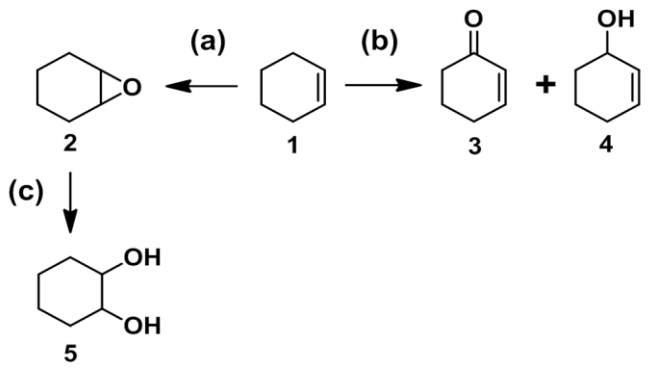

Scheme 1. Oxidation of cyclohexene **1** towards the main reaction products: (a) epoxidation to cyclohexene oxide **2**,(b) allylic oxidation to 2-cyclohexene-1-one **3** and 2-cyclohexen-1-ol **4**, (c) consecutive ring opening to cyclohexane-1,2-diol **5**.

Table 1. Results of the epoxidation of cyclohexene catalyzed by Cu based compounds

Catalyst		Conv. %	Selec.%	TOF h^{-1}	Leaching %	by-product Selec. %		
						3[c]	**4**[c]	**5**[c]
Cu^{2+}@COMOC-4[a]	1st run	49.0	89,0	21.5	0	4.3	2.6	3.9
	2nd run	46.2	87,0	19.7	0	5.3	3.1	4.5
	3rd run	41.5	87.8	18.9	0	5.6	3.1	3.4
	4th run	41.6	89.2	18.0	0	5.1	2.7	2.9
Cu-BTC		41.7	77.5	11.1	13.2	6.9	8.5	7.0
COMOC-4[b]		11.4	52.5	2.7	0			

[a] Reaction conditions: Cu^{2+}@COMOC-4 (0.19g in the 1st run, 0.2mmol Cu sites), chloroform (40 ml), substrate (7ml), isobutyraldehyde (11.4ml), O_2 (7.7 ml/min), tempt.=313 K, time=7 h. [b] Based on Cu^{2+}@COMOC-4, the equal amount of Ga sites (0.65mmol) were used, TOF were calculated based on the number of moles of Cu sites. [c] Referring to Scheme 1 for product distributions.

As presented in Table 1, both Cu-based catalysts, gave cyclohexene oxide as the predominant product (Scheme 1, pathway a). The Cu^{2+}@COMOC-4 shows a remarkable catalytic activity, affording 49% of cyclohexene conversion after 7 hours of catalysis with a selectivity of 89% towards the epoxide in the 1st run (Figure S4. supporting information). For the latter catalyst no leaching of Cu and Ga sites was detected during the first run, indicating that the catalysis occurs truly heterogeneous. In contrast to Cu^{2+}@COMOC-4, Cu-BTC, although the XRD pattern indicates after catalysis, no obvious changes in crystallinity (Figure S5 supporting information), a rather high Cu leaching of 13.2% was detected after catalysis, which clearly demonstrates that the catalytic activity of Cu-BTC is mainly due to homogeneous catalysis.

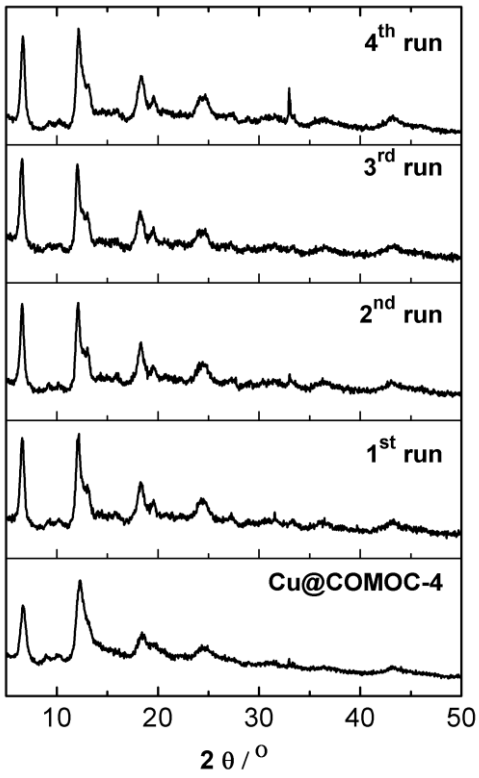

Figure 8. The XRD pattern of Cu^{2+}@COMOC-4 before and after each run of the catalysis cycles. (The peak at 32.9° is due to the background of the silicon sample holder)

Additionally, the recyclability and stability of the Cu^{2+}@COMOC-4 material was evaluated. In total, four successive runs were performed on Cu^{2+}@COMOC-4. The results of the consecutive runs are presented in Table 1 as well as in Figure S6, supporting information. Although there is a slight reduction in the cyclohexene conversion during the additional runs, the TOF value remains fairly constant. This observation demonstrates the good recyclability of the Cu^{2+}@COMOC-4 material. The slight decrease in the observed cyclohexene conversion is probably due to a small loss of catalyst after each run. Moreover, the selectivity towards the epoxide stays fairly constant in the additional runs. Besides cyclohexane-1,2 diol, which is the result of the opening of the epoxide due to the presence of trace amounts of water adsorbed on the hydrophilic MOFs, 2-cyclohexen-1-ol and 2-cyclohexen-1-one are the observed by-products during each catalytic test. The formation of the latter products is due to the allylic oxidation of

cyclohexene.[12c, 18a, 18b] No leaching of Cu and Ga species were observed during these successive runs, which demonstrates the stability and regenerability of the catalyst. In Figure 8, the XRPD pattern of the Cu^{2+}@COMOC-4 catalyst before and after each consecutive run is presented. From this figure it can be seen that the structural integrity of the framework is well preserved during these 4 following runs.

The Cu-BTC catalyst, which also contains unsaturated Cu sites, exhibits a similar product distribution and cyclohexene conversion (41.7% for Cu-BTC and 49% for Cu^{2+}@COMOC-4), however, a difference in selectivity was detected between both catalysts. In contrast to Cu^{2+}@COMOC-4, which has an average selectivity of 89% towards the epoxide, the Cu-BTC exhibits a lower selectivity of 77.5 % towards cyclohexene oxide, due to the formation of a larger amount of by-products (**3, 4** and **5**). This could be due to the different structure of the Cu-MOF in comparison to the Cu^{2+}@COMOC-4 material. The copper paddle-wheel units in Cu-BTC contain unsaturated Cu sites which are in favor of binding water molecules. The presence of this adsorbed water can play a prominent role in the ring opening of the epoxide.[19a, 19b, 19c] Moreover, the paddlewheel structure has been shown to have a catalytic influence on epoxide ring-opening reactions. [19b]

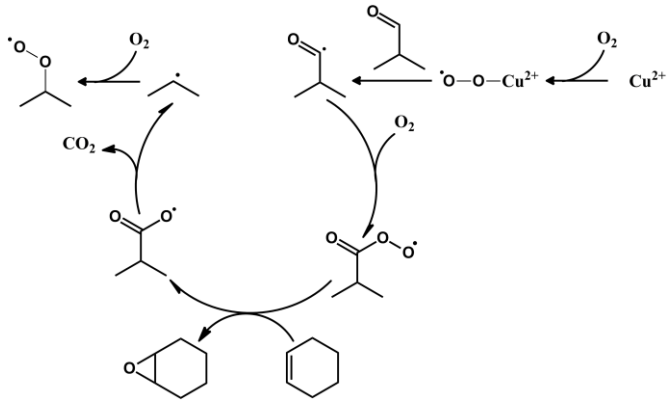

Scheme 2. Main mechanism to catalyse the cyclohexene epoxidation in the presence of molecular oxygen and isobutyraldehyde.

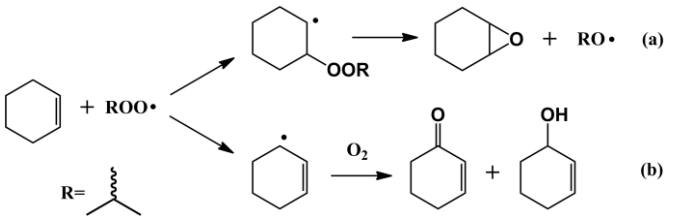

Scheme 3. The alkylperoxy radicals generated in the main catalytic cycle lead to the formation of by-products (b) next to the cyclohexene oxide (a). Adapted from ref [18a]

The reaction mechanism for the transition-metal-catalyzed aerobic oxidation of alkenes in the presence of an aldehyde as co-reagent is widely known in literature as the Mukaiyama-Yamada epoxidation reaction (see Scheme 2).[17] In this study, the autoxidation of the aldehyde plays a critical role in the catalytic process. Without the aldehyde, the Cu^{2+} catalysed alkene reaction are more in favor of allylic reaction pathway.[16e, 20] The co-reactant isobutyraldehyde is transformed in situ into an acylperoxy radical, which is the predominant oxidizing species, facilitating the oxygen transfer to the olefin. It should be noted that cyclohexene is a good substrate to investigate whether the oxidizing species prefers allylic oxidation or epoxidation.[18a, 18b] The acylperoxy radicals preferentially react with the double bond of the alkenes yielding the epoxide, as shown in Scheme 3. The latter pathway is the major reaction pathway observed during our catalytic tests indicating that the Cu^{2+} active sites mainly stabilize the acylperoxy radical. Afterwards, the unstable carboxyl radical decomposes, forming an alkyl radical, which can in turn be oxidized to an alkylperoxy radical. This species is less selective towards the formation of epoxides and leads to the formation of by-products via the allylic oxidation pathway (Scheme 3, pathway (b)).

Conclusion

A gallium based MOF, denoted as COMOC-4, has been successfully synthesized and characterized. In a second step $CuCl_2$ was incorporated into COMOC-4 by a post-modification approach. The successful incorporation was verified with the aid of ab initio techniques. The catalytic performance of the resulting Cu^{2+}@COMOC-4 was investigated for the aerobic oxidation of cyclohexene in the presence of the co-oxidant isobutyraldehyde. In comparison to Cu-BTC, Cu^{2+}@COMOC-4 shows the best catalytic performance in terms of selectivity towards cyclohexene oxide. Furthermore, no leaching of both Ga and Cu species was detected during 4 successive runs, indicating the good stability and reusability of the catalyst.

Experimental Section

General

The 2,2'-bipyridine-5,5'-dicarboxylic acid (H_2bpydc) ligand was prepared according to a procedure published elsewhere.[21] The commercially available spectroscopic grade methanol was applied for the spectroscopic studies. All the other starting materials (analytical grade) were bought and used without further purification. Cu-BTC (Basolite™ C300, Sigma-Aldrich) was activated at 120 °C under vacuum for 3 h prior to use.

Synthesis

Synthesis of the Cu complex: $[Cu(Me_2bpydc)]Cl_2(H_2O)_{1.5}$

The dimethyl [2,2'-bipyridine]-5,5'-dicarboxylate (Me_2bpydc) ligand was synthesized according to the procedure described by Gunyar et al.[22]. In a second step, 0.03g Me_2bpydc and 0.019g $CuCl_2{\cdot}2H_2O$ were mixed in a pyrex tube with 5ml of methanol. The pyrex tube was subsequently heated to 120°C and kept at this temperature overnight. Hereafter, the blue colored powder was filtered off, washed with acetone and dried under vacuum. Calcd for $CuCl_2((CH_3)_2(C_{12}H_6O_4N_2){\cdot}1.5H_2O$: C:41.49; H:2.70; N:6.24 Found: C:41.24; H:2.90; N:6.77.

Synthesis of COMOC-4 (Ga(OH)(bpydc))

The synthesis of COMOC-4 was optimized at the gram scale based on our earlier reported synthesis procedure.[10] $Ga(NO_3)_3{\cdot}H_2O$ (1.2 g, 4.4 mmol) and H_2bpydc (1.2g, 5mmol) were added to 120 mL DMF in a 250 mL schlenk flask equipped with a magnetic stirrer. In first instance, the mixture was heated to 110°C and kept at this temperature for 0.5 h. Afterwards the mixture was additionaly heated to 150 °C and held at this temperature for 48 h under mild stirring.

Hereafter, a orange-colored powder was collected over a membrane filter and washed thoroughly with respectively DMF, methanol and acetone. For the removal of unreacted linker from the pores, the solid product was suspended in DMF (0.5 g per 50 ml DMF), heated at 80 ^{o}C for 2 h, filtered off, washed with respectively DMF and acetone and dried under vacuum. In order to ensure a complete exclusion of the organic species encapsulated within the pores of the open framework, a Soxhlet extraction in methanol was carried out during 48 h at 120 ^{o}C. Afterwards the COMOC-4 material was dried under vacuum overnight at room temperature. Due to the presence of the –OH moiety on the gallium building unit, the 1D channels are highly hydrophilic. For this reason, the activated sample was stored under an inert atmosphere. The yield was 33% based on the gallium source. IR spectrum (cm^{-1}, KBr pellet): 3379 (br), 1619 (s), 1595 (s), 1421 (s), 1394 (s), 1158 (w), 1050 (w), 847 (w), 775(m), 705 (w), 600 (w), 479 (w). Calcd for Ga(OH)($C_{12}H_6N_2O_4$)·2.7H_2O: C, 38.36; H, 3.27; N, 7.46; Found: C, 38.26; H, 3.12; N, 7.17.

Grafting the $CuCl_2$ complex on the COMOC-4 framework

Cu^{2+}@COMOC-4 was prepared by stirring 0.5g of Ga(OH)(bpydc) and 0.1g $CuCl_2$·2H_2O in 30 ml absolute methanol at 50 ^{o}C for 6 h. Afterwards the green MOF powder was filtered off and was stirred an additional time in 20 ml pure methanol for 6 h followed by filtration. This procedure was repeated two times to guarantee the complete removal of physisorbed $CuCl_2$ salts.

Characterization

X-ray powder diffraction measurements and thermal gravimetric analysis

X-ray powder diffraction (XRPD) patterns were recorded on a Thermo Scientific ARL X'Tra diffractometer, operated at 40 kV, 40 mA using Cu-Kα radiation (λ = 1.5406 Å). Thermal gravimetric analysis (TGA) data were obtained on a Netzsch STA 449 F3 Jupiter-Simultaneous TG-DSC analyzer with a heating rate of 10 ˚C min^{-1} in air. N_2 sorption measurements were carried out on a Belsorp II, Bell Japan, Inc. All the samples were activated under vacuum at 120 ^{o}C for 3 h prior to analysis.

Spectroscopic characterizations

Fourier transform infrared (FT-IR) spectra were recorded in the region of 400-4000 cm^{-1} on a Bruker EQUINOX 55 FTIR spectrometer. The ultraviolet-visible (UV/Vis) absorption spectra were collected on a Perkin–Elmer Lambda 950 UV/Vis spectrometer in the range of 260-900 nm. The spectra were recorded using fine suspensions of powder samples (COMOC-4 and Cu^{2+}@COMOC-4) in methanol. In a typical measurement, 4mg of powder sample was suspended in 3ml of methanol in an ultrasonic bath for 5 mins. The suspension was transferred to a 10 mm path length quartz cuvette to record the spectrum. The UV-Vis diffuse reflection spectra (DRS) experiments were carried out using Hitachi U-3000 UV/VIS Spectrophotometer with diffuse reflectance accessory (integrated sphere) for spectrophotometric measurements in the range of 350−800 nm. The spectra were converted using the Kubelka−Munk function. The X-Ray Fluorescence Spectrometry (XRF) measurements were performed on a Rigaku NexCG, Energy Dispersive X-ray Fluorescence (EDXRF) instrument.

Computational Methodology

Molecular dynamics (MD) simulations were carried out on the linker with and without Cu-coordination in a vacuum box of 20Å x 20Å x 20 Å using the CP2K package[23]. All DFT calculations were done using the Gaussian plane waves (GPW) method[24], with a DZVP basis set, GTH pseudopotentials[25a, 25b] and the BLYP functional. MD runs were conducted using the canonical (NVT) ensemble at 300K with a time step of 1 fs. A chain of five Nosé-Hoover thermostats was used to control the temperature. The system was first allowed to equilibrate after which a simulation of 20 ps was used for analysis. The "dynamic" UV/VIS spectra were obtained by taking 100 snapshots from the simulation on which vertical TD-DFT calculations were performed. This methodology has previously proven valuable for the simulation of absorption spectra[11a, 11b, 26]. An average optical spectrum was then obtained. The influence of the methanol solvent was included via a polarizable continuum model (PCM) model. All TD-DFT calculations were done with the Gaussian09[27] program using the B3LYP[28a, 28b] functional and a 6-311+G(g) Pople basis set. We previously demonstrated that the B3LYP functional is very efficient for these type of systems[10]. The effect of relativistic contributions is found to be small, full details are given in the supporting information.

Catalysis

The oxidation of cyclohexene was carried out in a 100 ml glass reactor equipped with a reflux condenser with a recirculating cooling at -4 ^{o}C. In a typical catalytic test, the reactor was loaded with 0.19 g Cu^{2+}@COMOC-4 (0.2 mmol Cu active sites), 7 ml cyclohexene (5mmol), 11.4 ml isobutyraldehyde, 40 ml chloroform and 9 ml 1,2,4-trichlorobenzene employed as internal standard. The molar ratio cyclohexene/ co-oxidant (isobutyraldehyde) was 1/2. The O_2 flow rate was set to 7.7 ml per minute by means of a mass flow controller. All the catalytic tests were performed at a temperature of 40 °C. Blank reactions at this temperature showed no formation of oxidation products. During the catalytic tests, aliquots were gradually taken out of the mixture, diluted with 500 µl ethylacetate, and subsequently analyzed by GC–FID. The reaction products were identified with a TRACE GC×GC (Thermo, Interscience), coupled to a TEMPUS TOF-MS detector (Thermo, Interscience). The first column consists of a dimethyl polysiloxane package and has a length of 50 m, with an internal diameter of 0.25 mm, whereas the second column has a length of 2 m with an internal diameter of 0.15 mm. The package of the latter is a 50% phenyl polysilphenylene-siloxane. Helium was used as carrier gas with a constant flow (1.8 mL/min).

All the fresh catalysts were activated under vacuum at 120 ^{o}C for 3 h prior to catalysis. After each catalytic run, the catalyst was recovered by filtration, washed with acetone and dried at room temperature overnight under vacuum to reuse it in a next run. In order to investigate the recyclability of the Cu^{2+}@COMOC-4 catalyst, four consecutive runs were performed. Moreover, to examine the heterogeneity of the catalyst, the filtrate, after the removal of the catalyst, was analyzed by means of XRF to quantify the possibly leached Cu and Ga species.

Acknowledgements

The authors acknowledge the financial support from the Ghent University BOF Grant (Nr. 01P02911T), GOA Grant (01G00710) and the Long Term Structural Methusalem grant nr. 01M00409 Funding by the Flemish Government. Furthermore, this research is co-funded by BELSPO in the frame of IAP 6/27 and the European Research Council (FP7(2007-2013) ERC Grant (Nr. 240483). Computational resources and services were provided by Ghent University.

Keywords: ab initio simulations • aerobic • epoxidation • heterogeneous catalysis • metal organic framework

References

[1] a) Corma, A., J. Catal. 2003, 216 (1–2), 298-312; b) Clark, J. H.; Macquarrie, D. J., Org. Process Res. Dev. 1997, 1 (2), 149-162

[2] a) Long, J. R.; Yaghi, O. M., Chem. Soc. Rev. 2009, 38 (5), 1213-1214; b) Tanabe, K. K.; Cohen, S. M., Chemical Society Reviews 2011, 40 (2), 498-519; c) Rowsell, J. L. C.; Yaghi, O. M., Microporous and Mesoporous Materials 2004, 73 (1-2), 3-14

[3] a) Eddaoudi, M.; Moler, D. B.; Li, H. L.; Chen, B. L.; Reineke, T. M.; O'Keeffe, M.; Yaghi, O. M., Accounts of Chemical Research 2001, 34 (4), 319-330; b) Yaghi, O. M.; Li, H. L.; Davis, C.; Richardson, D.; Groy, T. L., Accounts of Chemical Research 1998, 31 (8), 474-484

[4] a) Dhakshinamoorthy, A.; Alvaro, M.; Garcia, H., Catalysis Science & Technology 2011, 1 (6), 856-867; b) Van Speybroeck, V.; Leus, K.; Muylaert, I.; Vandichel, M.; Marin, G. B.; Waroquier, M.; Van der Voort, P., Chem. Commun. 2010, 46 (28), 5085-5087; c) Corma, A.; Garcia, H.; Llabres i Xamena, F. X., Chem. Rev. 2010, 110 (8), 4606-4655

[5] a) Ma, L.; Falkowski, J. M.; Abney, C.; Lin, W., Nat. Chem. 2010, 2 (10), 838-846; b) Carson, F.; Agrawal, S.; Gustafsson, M.; Bartoszewicz, A.; Moraga, F.; Zou, X.; Martin-Matute, B., Chemistry-a European Journal 2012, 18 (48), 15337-15344; c) Leus, K.; Vanhaelewyn, G.; Bogaerts, T.; Liu, Y.-Y.; Esquivel, D.; Callens, F.; Marin, G. B.; Van Speybroeck, V.; Vrielinck, H.; Van Der Voort, P., Catal. Today (0),

[6] Leus, K.; Vanhaelewyn, G.; Bogaerts, T.; Liu, Y.-Y.; Esquivel, D.; Callens, F.; Marin, G. B.; Van Speybroeck, V.; Vrielinck, H.; Van Der Voort, P., Catal. Today 2013, 208 (0), 97-105

[7] Bloch, E. D.; Britt, D.; Lee, C.; Doonan, C. J.; Uribe-Romo, F. J.; Furukawa, H.; Long, J. R.; Yaghi, O. M., J. Am. Chem. Soc. 2010, 132 (41), 14382-14384

[8] Carson, F.; Agrawal, S.; Gustafsson, M.; Bartoszewicz, A.; Moraga, F.; Zou, X.; Martín-Matute, B., Chemistry – A European Journal 2012, 18 (48), 15337-15344

[9] Wang, M.; Yuan, B.; Ma, T.; Jiang, H.; Li, Y., RSC Advances 2012, 2 (13), 5528-5530

[10] Liu, Y.-Y.; Decadt, R.; Bogaerts, T.; Hemelsoet, K.; Kaczmarek, A. M.; Poelman, D.; Waroquier, M.; Van Speybroeck, V.; Van Deun, R.; Van Der Voort, P., The Journal of Physical Chemistry C 2013, 117 (21), 11302-11310

[11] a) De Meyer, T.; Hemelsoet, K.; Van der Schueren, L.; Pauwels, E.; De Clerck, K.; Van Speybroeck, V., Chemistry – A European Journal 2012, 18 (26), 8120-8129; b) Barone, V.; Bloino, J.; Monti, S.; Pedone, A.; Prampolini, G., Phys. Chem. Chem. Phys. 2010, 12 (35), 10550-10561

[12] a) Monteiro, B.; Gago, S.; Balula, S. S.; Valente, A. A.; Gonçalves, I. S.; Pillinger, M., J. Mol. Catal. A: Chem. 2009, 312 (1–2), 23-30; b) Nandi, M.; Roy, P.; Uyama, H.; Bhaumik, A., Dalton Trans. 2011, 40 (46), 12510-12518; c) Komiya, N.; Naota, T.; Oda, Y.; Murahashi, S.-I., J. Mol. Catal. A: Chem. 1997, 117 (1–3), 21-37

[13] Senkovska, I.; Hoffmann, F.; Froba, M.; Getzschmann, J.; Bohlmann, W.; Kaskel, S., Microporous Mesoporous Mater. 2009, 122 (1-3), 93-98

[14] a) Loiseau, T.; Serre, C.; Huguenard, C.; Fink, G.; Taulelle, F.; Henry, M.; Bataille, T.; Ferey, G., Chem-Eur J 2004, 10 (6), 1373-1382; b) Jacobson, A. J.; Vougo-Zanda, M.; Huang, J.; Anokhina, E.; Wang, X. Q., Inorg. Chem. 2008, 47 (24), 11535-11542

[15] Carson, F.; Agrawal, S.; Gustafsson, M.; Bartoszewicz, A.; Moraga, F.; Zou, X. D.; Martin-Matute, B., Chem. Eur. J. 2012, 18 (48), 15337-15344

[16] a) Beier, M. J.; Kleist, W.; Wharmby, M. T.; Kissner, R.; Kimmerle, B.; Wright, P. A.; Grunwaldt, J.-D.; Baiker, A., Chemistry – A European Journal 2012, 18 (3), 887-898; b) Dhakshinamoorthy, A.; Alvaro, M.; Garcia, H., J. Catal. 2012, 289 (0), 259-265; c) Maksimchuk, N. V.; Kovalenko, K. A.; Fedin, V. P.; Kholdeeva, O. A., Chem. Commun. 2012, 48 (54), 6812-6814; d) Balu, A. M.; Lin, C. S. K.; Liu, H.; Li, Y.; Vargas, C.; Luque, R., Applied Catalysis A: General 2013, 455 (0), 261-266; e) Luz, I.; Leon, A.; Boronat, M.; Llabres i Xamena, F. X.; Corma, A., Catalysis Science & Technology 2013, 3 (2), 371-379; f) Skobelev, I. Y.; Sorokin, A. B.; Kovalenko, K. A.; Fedin, V. P.; Kholdeeva, O. A., J. Catal. 2013, 298 (0), 61-69

[17] Takai, T.; Yamada, T.; Mukaiyama, T., Chem. Lett. 1991, (9), 1499-1502

[18] a) Wentzel, B. B.; Alsters, P. L.; Feiters, M. C.; Nolte, R. J. M., J. Org. Chem. 2004, 69 (10), 3453-3464; b) Nam, W. W.; Kim, H. J.; Kim, S. H.; Ho, R. Y. N.; Valentine, J. S., Inorg. Chem. 1996, 35 (4), 1045-1049

[19] a) Bao, H. L.; Zhou, J.; Wang, Z.; Guo, Y. L.; You, T. P.; Ding, K. L., J. Am. Chem. Soc. 2008, 130 (31), 10116-10127; b) Tanaka, K.; Otani, K.; Murase, T.; Nishihote, S.; Urbanczyk-Lipkowska, Z., Bull. Chem. Soc. Jpn. 2012, 85 (6), 709-714; c) Vilotijevic, I.; Jamison, T. F., Science 2007, 317 (5842), 1189-1192

[20] Fu, Y.; Sun, D.; Qin, M.; Huang, R.; Li, Z., Rsc Advances 2012, 2 (8), 3309-3314

[21] Szeto, K. C.; Kongshaug, K. O.; Jakobsen, S.; Tilset, M.; Lillerud, K. P., Dalton Trans. 2008, (15), 2054-2060

[22] Gunyar, A.; Betz, D.; Drees, M.; Herdtweck, E.; Kuhn, F. E., Journal of Molecular Catalysis a-Chemical 2010, 331 (1-2), 117-124

[23] http://cp2k.berlios.de/,

[24] Lippert, G.; Hutter, J.; Parrinello, M., Mol. Phys. 1997, 92 (3), 477-487

[25] a) Goedecker, S.; Teter, M.; Hutter, J., Phys. Rev. B 1996, 54 (3), 1703-1710; b) Hartwigsen, C.; Goedecker, S.; Hutter, J., Phys. Rev. B 1998, 58 (7), 3641-3662

[26] Adamo, C.; Jacquemin, D., Chem. Soc. Rev. 2013, 42 (3), 845-856

[27] M. J. Frisch, G. W. Trucks, H. B. Schlegel, G. E. Scuseria, M. A. Robb, J. R. Cheeseman, G. Scalmani, V. Barone, B. Mennucci, G. A. Petersson, H. Nakatsuji, M. Caricato, X. Li, H. P. Hratchian, A. F. Izmaylov, et al. Gaussian 09, Revision A.02, Gaussian, Inc., Wallingford CT; 2009.

[28] a) Becke, A. D., J. Chem. Phys. 1993, 98 (7), 5648-5652; b) Lee, C. T.; Yang, W. T.; Parr, R. G., Phys. Rev. B 1988, 37 (2), 785-789

Received: ((will be filled in by the editorial staff))
Published online: ((will be filled in by the editorial staff))

Entry for the Table of Contents

FULL PAPER

MOF with craws: COMOC-4, a gallium based metal-organic framework was synthesized containing open bipyridine sites on which $CuCl_2$ was anchored. The catalytic performance of the resulting Cu^{2+}@COMOC-4 was evaluated for the aerobic oxidation of cyclohexene. The bimetallic-organic framework shows an excellent selectivity towards cyclohexene oxide and exhibited a good stability and reusability.

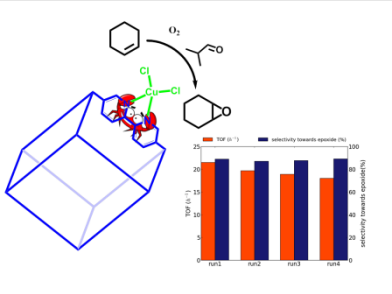

*Ying-Ya Liu, Karen Leus, Thomas Bogaerts, Karen Hemelsoet, Els Bruneel, Veronique Van Speybroeck and Pascal Van Der Voort**

Page No. – Page No.

Cu^{2+}@COMOC-4: a bimetallic-organic framework as zero-leaching catalyst in the aerobic oxidation of cyclohexene

Supporting information for

Cu^{2+}@COMOC-4: a bimetallic-organic framework as zero-leaching catalyst in the aerobic oxidation of cyclohexene

Ying-Ya Liu, [a] Karen Leus, [a] Thomas Bogaerts, [a, b] Karen Hemelsoet, [b] Els Bruneel, [c] Veronique Van Speybroeck[b] and Pascal Van Der Voort*[a]

[a] *COMOC - Center for Ordered Materials, Organometallics and Catalysis, Department of Inorganic and Physical Chemistry, Ghent University, Krijgslaan 281-S3, 9000 Ghent; Belgium*

[b] *Center for Molecular Modeling, Ghent University, Technologiepark 903, 9052 Zwijnaarde, Belgium*

E-mail: pascal.vandervoort@ugent.be

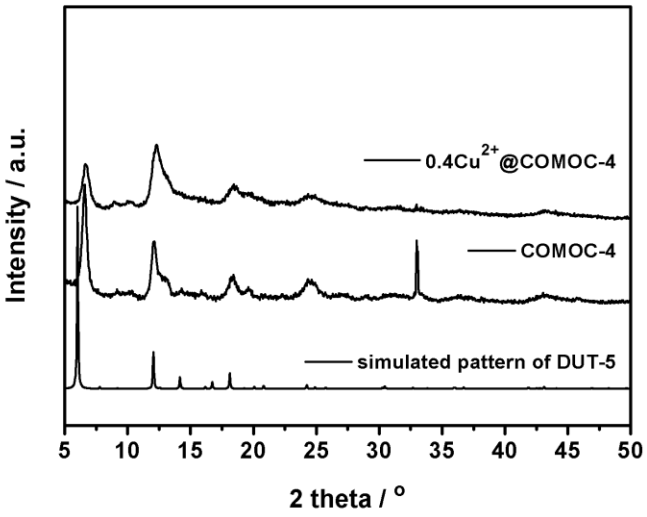

Figure S1 Powder XRD patterns of COMOC-4, Cu^{2+}@COMOC-4 compared with simulated pattern of Al(OH)(BPDC) (DUT-5, $BPDC^{2-}$= 2,2'-biphenyl-5,5'-dicarboxylate) (The peak at 32.9 °is due to the background of the silicon sample holder).

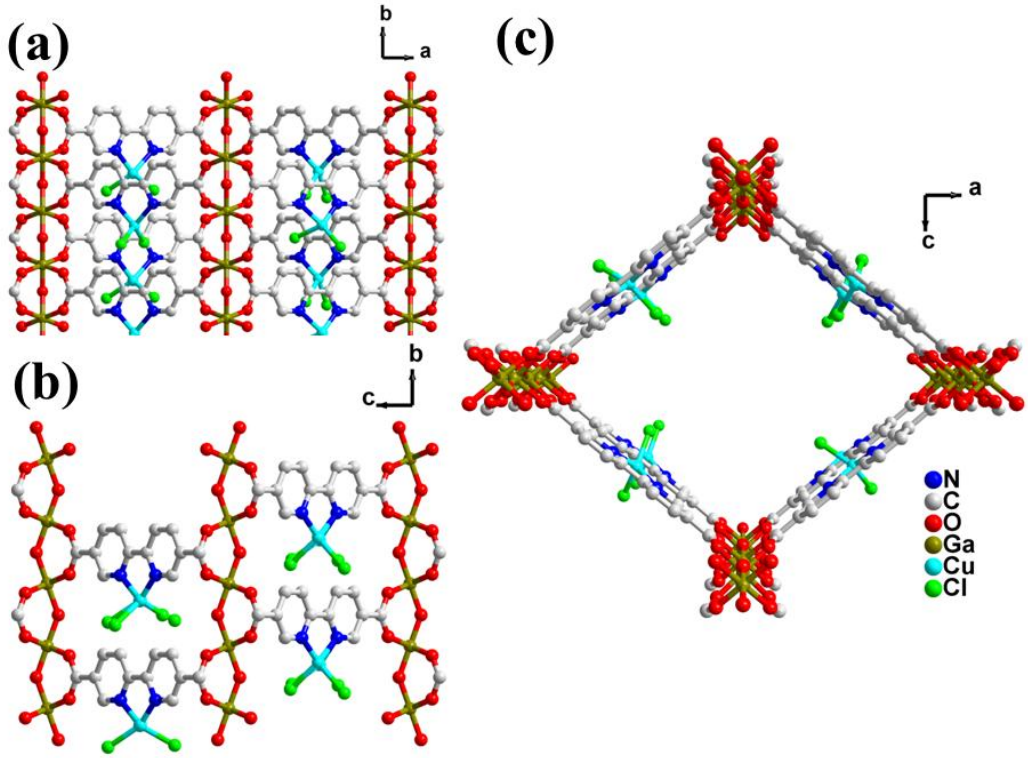

Figure S2 Representative structure of Cu^{2+}@COMOC-4. View perpendicular to (a,b) and along (c) the one dimensional pore system. The structure model was generated based on the crystal structure of DUT-5. [1].

Influence of metal coordination on the computed spectra – Metal-to-ligand character

In order to determine if the changes in the calculated UV/Vis spectrum are a consequence of the metal coordination, the molecular orbitals corresponding to the extra bands in the absorption spectrum were visualized. Figure S3(a) displays the theoretical UV/Vis spectrum of a the cupper-modified linker. The spectrum was calculated for the optimized geometry using TD-DFT, in particular B3LYP/6-311+G(d).

Three peaks can be distinguished, with maxima around 403, 324 and 307 nm. These values deviate from the values of the averaged MD spectrum (see Figure 4 in the main manuscript) since it corresponds with one particular geometry, however the overall shape of the spectrum is maintained. This behavior is explained in more detail in refs.[2a, 2b]

We focus on the absorption at 403 and 324 nm, which are due to the metal coordination. Investigation of the underlying transitions reveals that a variety of orbitals is involved. However, the feature at 403 nm mainly results from a HOMO to LUMO transition (in particular orbitals 103a and 104a are involved, see Figure S3(b)). The peak at 324 nm is mainly due to a transition from orbital 100a to 104a as well as from 100b to 104b (Figure S3(c)). The involved orbitals are depicted and the participation of the $CuCl_2$ and linker fragments in the oribitals are also given. From this information, it is clear that the observed peaks involve a metal-to-ligand transition.

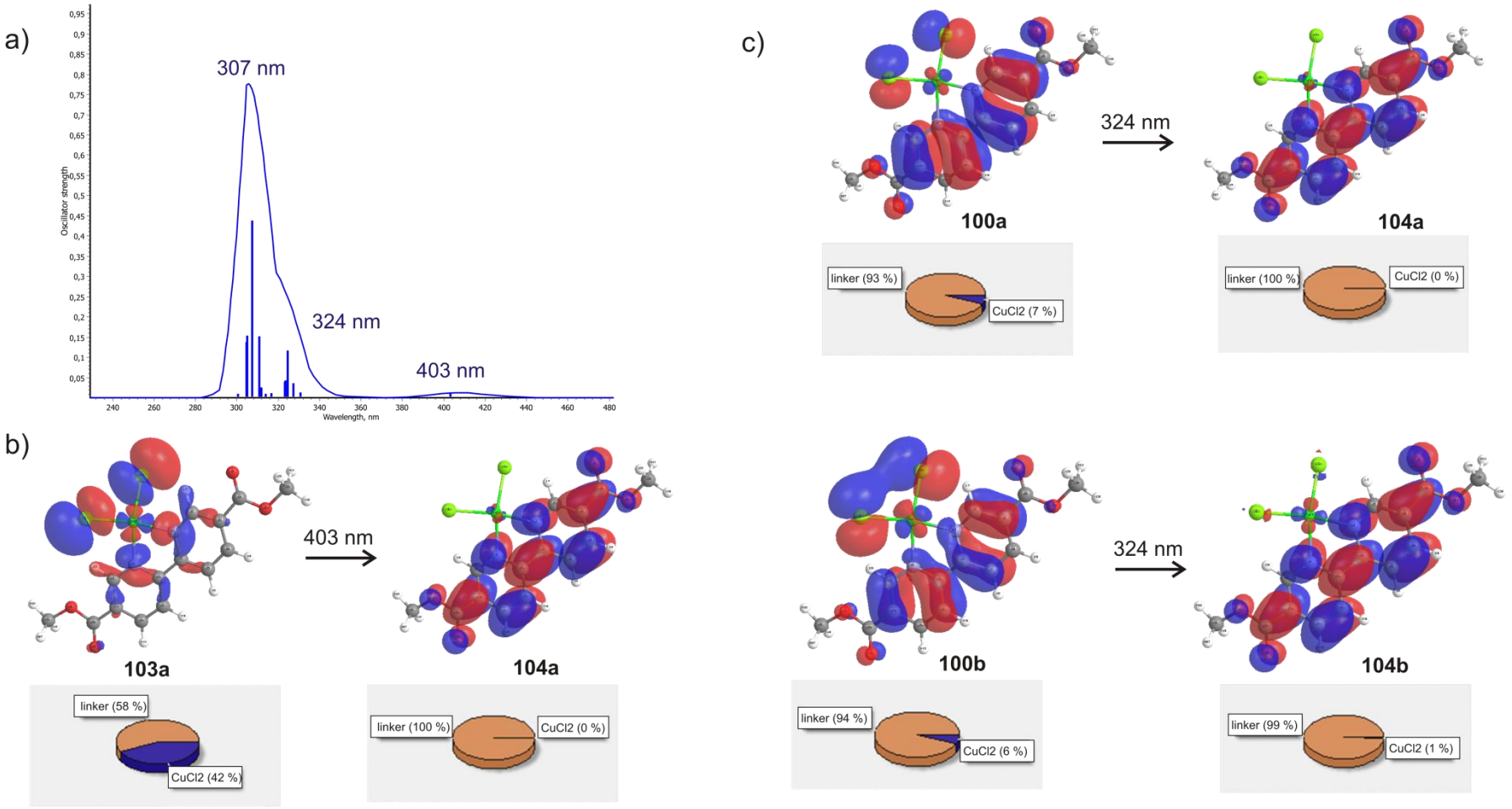

Figure S3 (a) Theoretical UV/Vis spectrum of the Cu-modified linker, calculated for a snapshot extracted from the MD simulation. (b) Iso-surfaces of dominant orbitals involved in the excitation at 403 nm. (c) Iso-surfaces of the dominant orbitals involved in the excitation at 324 nm.The participation of the separate fragments are also depicted; in particular in orange for the linker and in blue for the $CuCl_2$.

Influence of relativistic effects on the theoretical simulations of the Cu-modified linker

All TD-DFT simulations are done using the B3LYP/6-311+G(d) level of theory. We believe this method is adequate to model the systems under investigation, since we are aiming at describing the difference between the parent and modified linker. In this light, we refer to a study of Ghost et al.,[3] who report on the successful use of B3LYP with a standard basis set on copper complexes for TDDFT calculations.

However, relativistic contributions are necessary when results of high quantitative accuracy are targeted. To assess the influence of relativistic contributions on our results, additional simulations were performed using the Orca program. Relativistic effects were explicitly taken into account using the ZORA option. This methodology is similar to the one used by Ji et al. [4] for the simulation of luminescent properties of MOF-5.

Table S1 lists the important absorption peaks of the Cu-modified linker. In addition to testing the influence of relativistic effects, also the performance of two basis sets (in particular SVP and TZVPP) and the BLYP and B3LYP functionals were assessed. This is necessary, since a straightforward comparison with the original results is not straightforward due to the use of different software packages and implementations. We note that in the computed spectra a large number of excitations, with small oscillator strengths, is observed. The results in Table S1 correspond to the excitations with maximal oscillator strength in the region of interest (between 400-480 nm). We indeed observe a substantial shift between the values computed using the Gaussian (403nm; Figure S3) and Orca (close to 450 nm; Table S1) programs. The values of Table S1 are in closer agreement with the averaged MD result (see Figure 4 of the main manuscript); a full analysis is however outside the scope of this paper.

Table S1. Computed excitation energies [in nm] for the Cu-modified bipyridine linker.

	Cu-bipyridine			
	BLYP		B3LYP[a]	
	Without ZORA	With ZORA	Without ZORA	With ZORA
SVP	454	457	460	453
TZVPP[a]	453	452	-	-

[a] The B3LYP/TZVPP simulations are computationally too demanding for the Cu-modified linker

Importantly, the additional simulations support the observation that relativistic effects do not substantially change the qualitative behavior of the optical spectrum of the Cu-modified linker, a maximal shift of 7 nm is obtained between the results with and without ZORA effects. This conclusions suggests that the original methodology (i.e. TD-DFT simulations using the B3lYP/6-311+G(d) level of theory) succeeds at describing the systems under investigation.

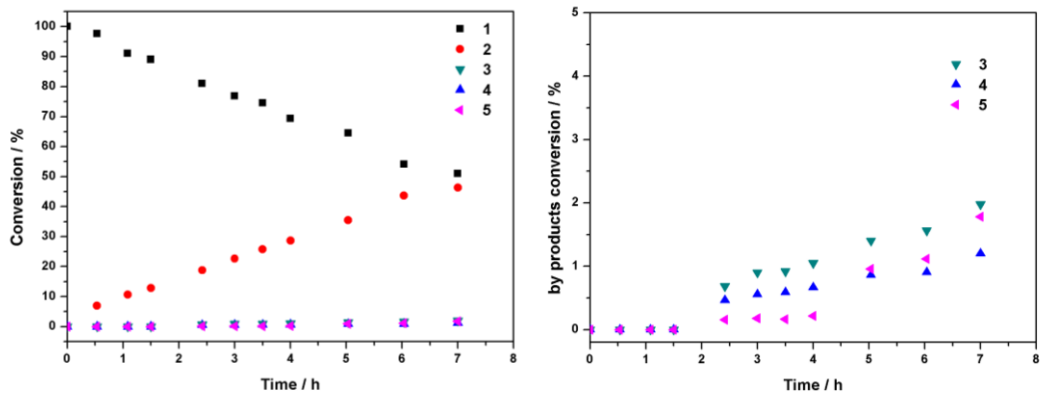

Figure S4 Left: Time conversion of cyclohexene (**1**) and time evolution of product distribution (cyclohexene oxide (**2**), 2-cyclohexene-1-one (**3**), 2-cyclohexen-1-ol (**4**) and cyclohexane-1,2-diol (**5**)) over Cu^{2+}@COMOC-4 during the 1st run. Right: detailed time evolution of by-product distribution over Cu^{2+}@COMOC-4 during the 1st run.

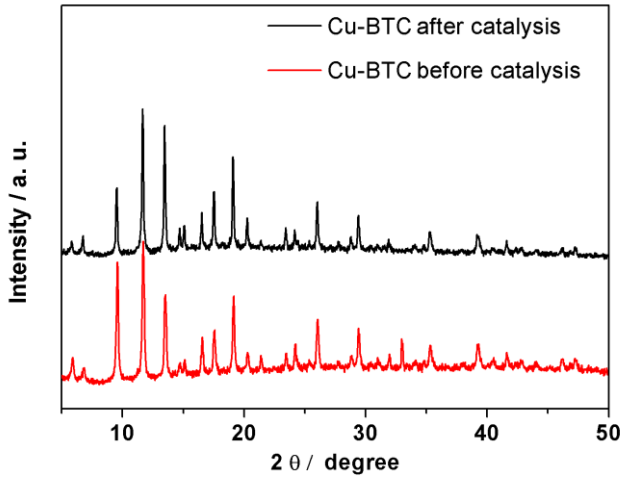

Figure S5 XRD comparison of Cu-BTC before and after catalysis.

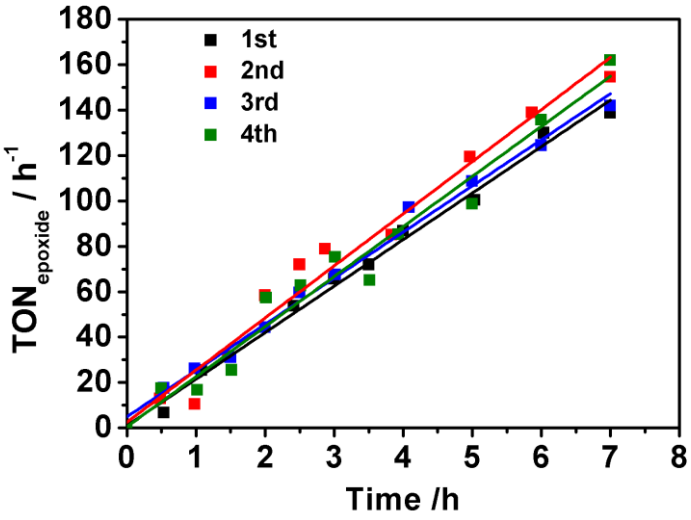

Figure S6 The catalytic activity expressed as TON for Cu^{2+}@COMOC-4 for 4 runs.

References

[1] Senkovska, I.; Hoffmann, F.; Froba, M.; Getzschmann, J.; Bohlmann, W.; Kaskel, S., *Microporous Mesoporous Mater.* **2009,** *122* (1-3), 93-98

[2] a) De Meyer, T.; Hemelsoet, K.; Van der Schueren, L.; Pauwels, E.; De Clerck, K.; Van Speybroeck, V., *Chem. - A Eur. J.* **2012,** *18* (26), 8120-8129; b) K. Hemelsoet, Q. Qian, T. De Meyer, K. De Wispelaere, B. De Sterck, B. M. Weckhuysen, M. Waroquier, V. Van Speybroeck, *Chem. - A Eur. J.* 2013, doi: 10.1002/chem.201301965

[3] Alemayehu, A.; Conradie, J.; Ghosh, A., *Eur. J. Inorg. Chem.* **2011,** *2011* (12), 1857-1864

[4] Ji, M.; Lan, X.; Han, Z.; Hao, C.; Qiu, J., *Inorg. Chem.* **2012,** *51* (22), 12389-12394